CHAPTER (3)

Results and Discussion

Within the aim of this thesis which is mainly to prepare and assess a suitable sorbent for the removal of uranium from the liquid waste produced from the Egyptian fuel manufacture pilot plant, FMPP. The results and discussion includes four main parts. The first address the preparation of the different sorbents and their characterization. The second part is concerned with the sorption investigations of uranium on the prepared sorbents and assessment for the choice of the recommended sorbent. Part three of this chapter is concerned with investigations on the liquid wastes produced from the FMPP facility and determination of uranium in these waste streams. Finally, part four addresses a development recommended procedure for separation of uranium from liquid wastes produced from the FMPP facility.

3.1 Preparation and Characterization of Sorbents.

In this work, two sorbents were prepared. The first is amidoxime chelating starch resin and the second is activated charcoal.

3.1.1 Preparation of amidoxime chelating starch resin

Chelating polymers based on graft polymerization of acrylonitrile monomer have attracted much attention for application in the adsorption of heavy metals. Preparation of these materials is based on two steps. The first step is by grafting acrylonitrile monomer on starch backbone and the second step is by treatment of the grafted nitrile polymer with hydroxylamine. In this thesis, two approached were investigated for graft polymerizations of acrylonitrile on starch. The first is based on chemical grafting and the second is based on radiation grafting.

3.1.1.1 Chemical grafting process

The mechanism of graft copolymerization of the acrylonitrile monomer onto starch macromolecules was proposed by Ceresa [149]. Here, the reaction of acrylonitrile monomer with starch initiated by ceric ion takes place in three steps and

the mechanism of the reaction of free-radical initiating process proceeds as the following steps in Schema[3.1].

Initiation

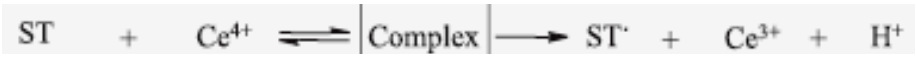

(1)

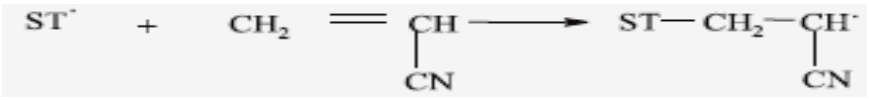

(2)

Where ST and ST is the sago starch and free radical of sago starch, respectively.

Propagation

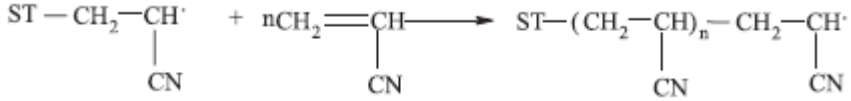

(3)

Termination

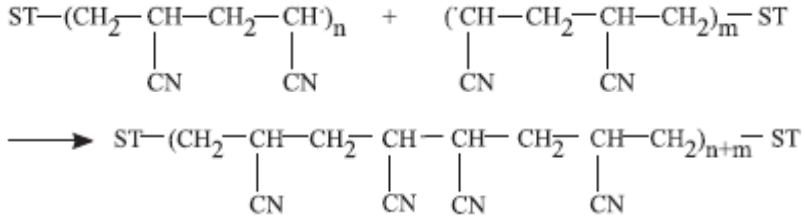

(4)

Scheme(3.1): The mechanism of graft copolymerization of the vinyl monomer onto starch (PAN copolymerization) using Free-radical initiating process

The first step in the polymerization process is the initiation of the backbone of the sorbent together with the formation of the free radical of the starch using tetravalent cerium according to equation 1 and 2. The starch obtained interacts with acrylonitrile monomer, equation 3, which is then prorogated and terminated, with other acrylonitrile monomers to form the nitrile polymer, equation 4, with the back bone of the starch.

As mentioned in the experimental, the aforementioned reactions were carried out by refluxing starch suspension in nitrogen atmosphere followed by the addition of dilute sulfuric acid and ceric ammonium nitrate as oxidizing agent. Graft polymerization of acrylonitrile was then obtained by adding the acrylonitrile monomer to obtain the nitrile polymer. The degree of grafting by this chemical

initiation was found rather small and equals 65%. This limits the applicability of this method of preparation for the amodoxime sorbent.

3.1.1.2 Radiation grafting Process

It is well established that ionizing radiation produce polymerization, therefore radiation grafting was used for polymerization of starch with acrylonitrile monomer. Within this merits, starch and acrylonitile monomer were irradiated by a dose of 15 kGy of the γ- ray from Co-60 source at a dose rate of 2.5 k Gy/h at the cyclotrone γ-Cell at the Nuclear Research Center, Egypt. This is illustrated in Schema (3.2).

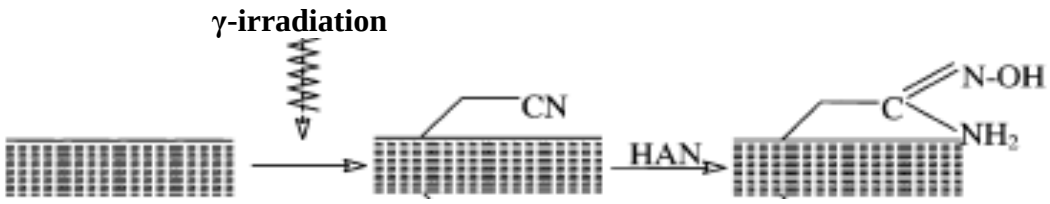

Schema (3.2): Preparation of chelating starch(amidoxime sorbent) by radiation-induced polymerization

Under theses conditions, the percent grafting reached 95%. This grafting value is much higher than that obtained by chemical grafting and therefore the different factors affecting radiation grafting was investigated in details.

It is to be mentioned that in the irradiation of the starch and the monomer mixture, the γ-rays on the starch brings radical formation. The sites of the radical formation become the points of initiation for side chains. At the time radiation initiates polymerization of the monomer and thus a mixture of graft copolymer and homopolymer is obtained. The homopolymerization increases with reaction time in competition with graft polymerization results in formation of homopolymer as an undesired by-product. In many studies inhibitors such as Cu and Fe salts are added to the grafting system to minimize the homopolymer by-products, but at the same time the grafting yield is also reduced in the presence of these scavengers. The metal ions diffuse into the swelling polymer matrix and terminate by growing grafted branches as well as growing homopolymer chains [150]. In this study Fe or Cu salts are not used in the grafting process because the presence of metal ions causes contamination

of the prepared chelating starch and makes it unacceptable for application in the adsorption process of radioactive elements. In addition, under suitable conditions of monomers concentration, composition, and radiation dose the grafted starch can be separated from the homopolymer in the purification step without using inhibitors. Also, an alternate method [150] using the styrene comonomer procedure was developed specially to overcome the limitations of Cu and Fe. In the presence of 10-20% styrene, the graft is almost completely composed of second monomer with little incorporation of styrene. The technique leads to a reduction in the propagation rate constant of the acrylonitrile in the presence of styrene.

It is known that the main factors affecting the irradiation process are the irradiation dose and the dose rate [151]. Therefore, the effect of radiation dose and dose rate were investigated.

The variation of grafting with radiation dose in graft polymerization of acrylonitrile solution onto starch and at a constant dose rate of 2.5 kGy/h is shown in Fig.(3.1). Grafting increases with radiation dose in the range from 0 to 20 kGy and then tends to level off above 15 kGy, i.e. the amount of radicals formed by radiation increases linearly with radiation dose and then reaches a certain limiting value at a higher doses. At higher irradiation doses the grafting tends to level off due to the recombination of some of the free radicals without initiating graft polymerization [152]. This leveling could be related to the fact that at higher levels of grafting, the reaction becomes a diffusion controlled process [153]. Grafting of acrylonitrile gives considerable grafting yields at suitable radiation doses of 15 kGy. Below and above these radiations, low grafting yield is obtained and removal of homopolymer becomes difficult, respectively.

Fig.(3.2) shows the degree of grafting vs. time for the grafting of acrylonitrile onto starch, at constant of radiation dose. It is observed that, the degree of grafting increases with grafting time. On the other hand, the grafting is inversely proportional to dose rate at constant dose. This indicated that the radiation doses of low rate (2 kGy/h) are better for grafting system than the same radiation dose of higher rate (2.5 kGy/h). At the selected monomers composition, the initial rate of grafting is relatively fast followed by a slower rate. This behavior is attributed to the consumption of the monomer, as well as to the reduction in the number of active sites on the starch backbone accessible for the grafting as the reaction proceeds [154].

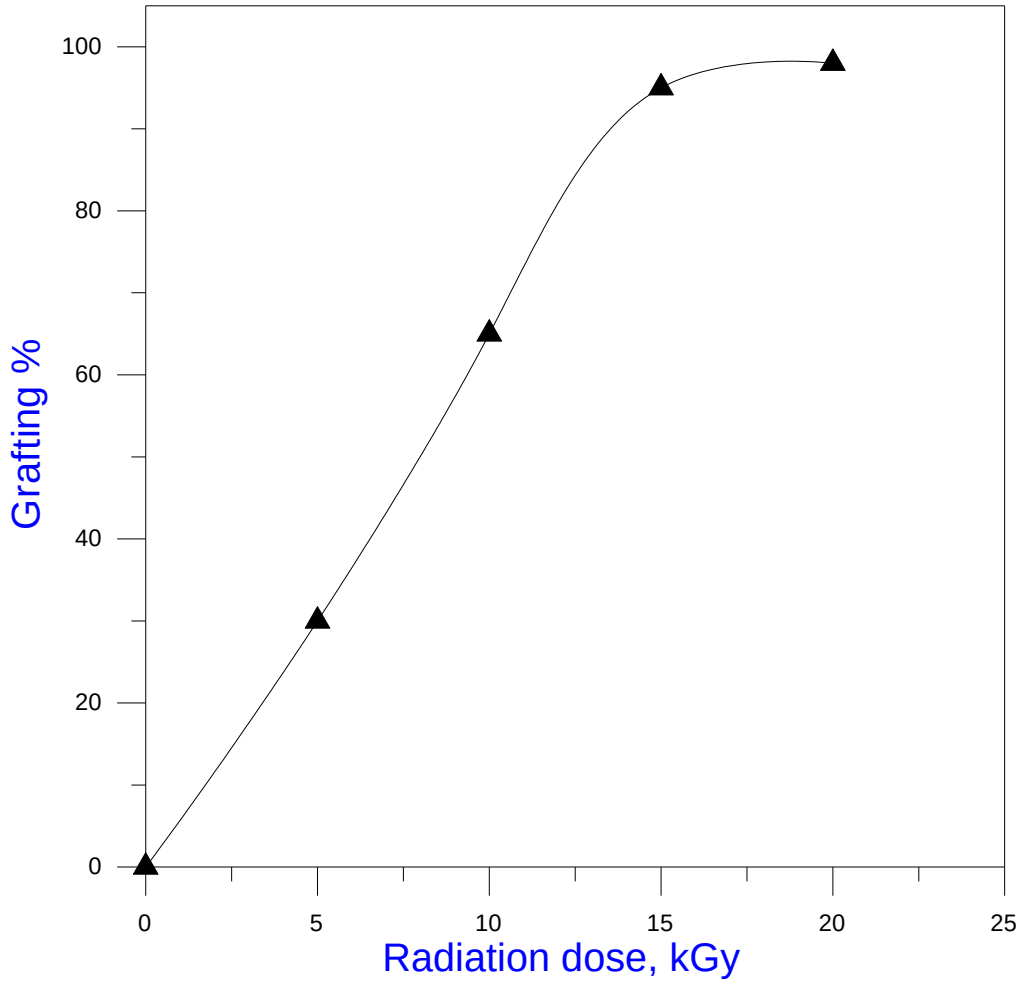

Fig (3.1): Effect of radiation dose in the grafting ratio, Dose rate 2.5 kGy/h.

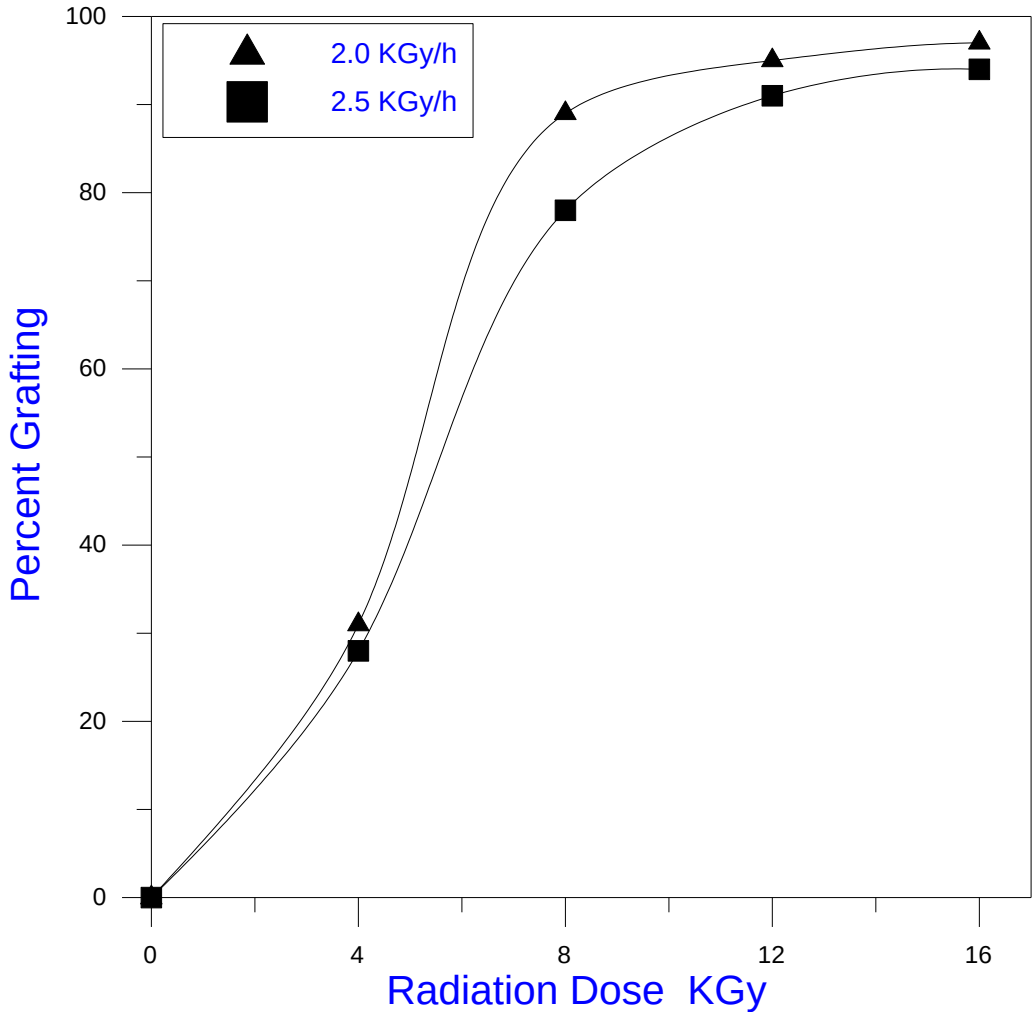

Fig (3.2): Effect of dose rate on the grafting % at constant radiation dose

3.1.1.3 Chemical Viz radiation grafting

It is of interest to compare chemical against radiation grafting processes for the system under investigation. The experimental results indicated that the grafting efficiency using radiation is much higher than that by chemical grafting. This was further documented by measuring the IR spectrum of the grafted polymer for the two samples, Fig 3.3 and Fig 3.4. From these figures it is clear that the spectrum obtained by radiation grafting is more defined with high intensity band for the nitrile group at 2245.9 cm^{-1}.

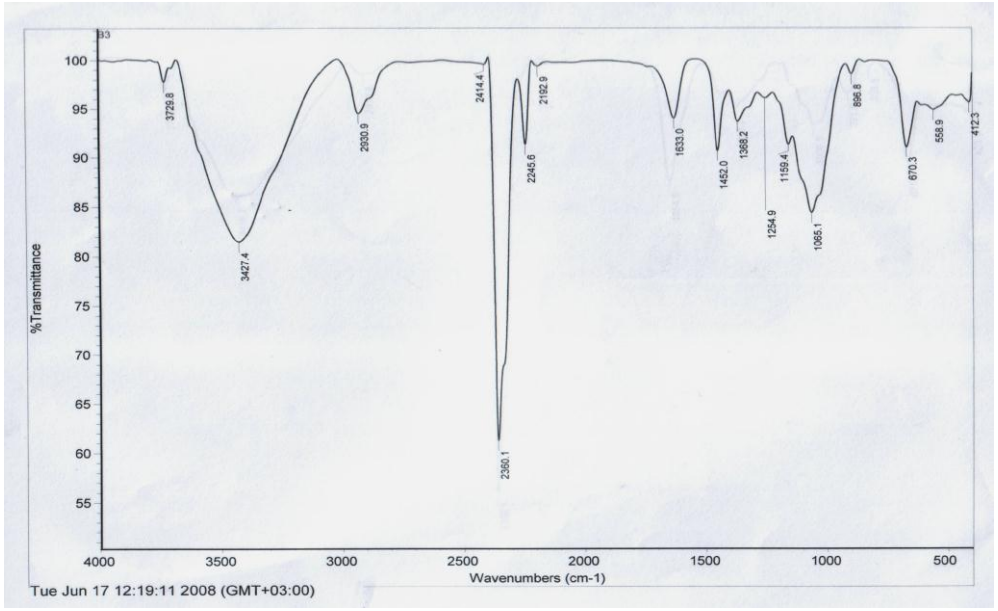

(a)

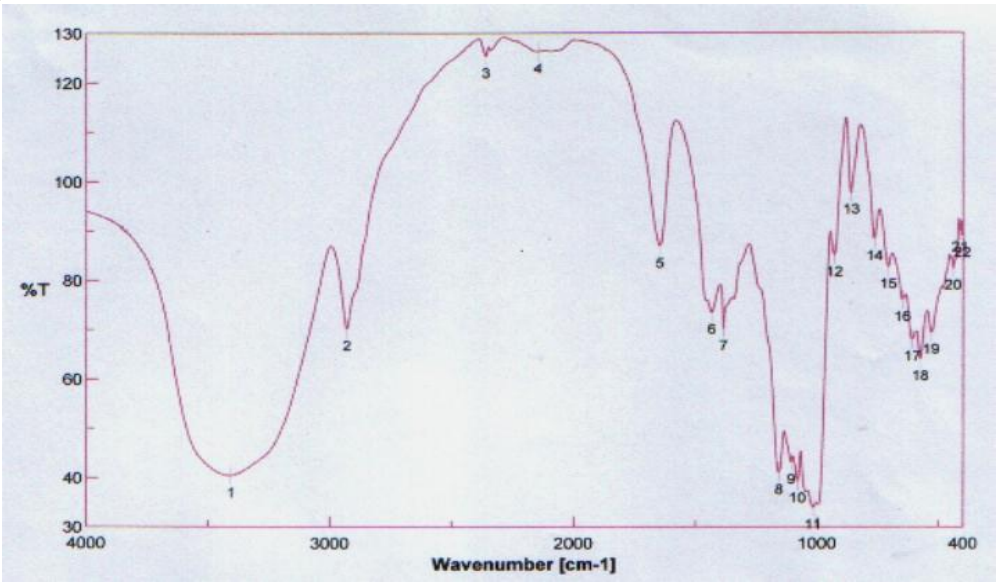

(b)

Fig (3.3): FT-IR spectra for PAN induced by (a) irradiation at radiation dose15 kGy (b)-chemical initiation.

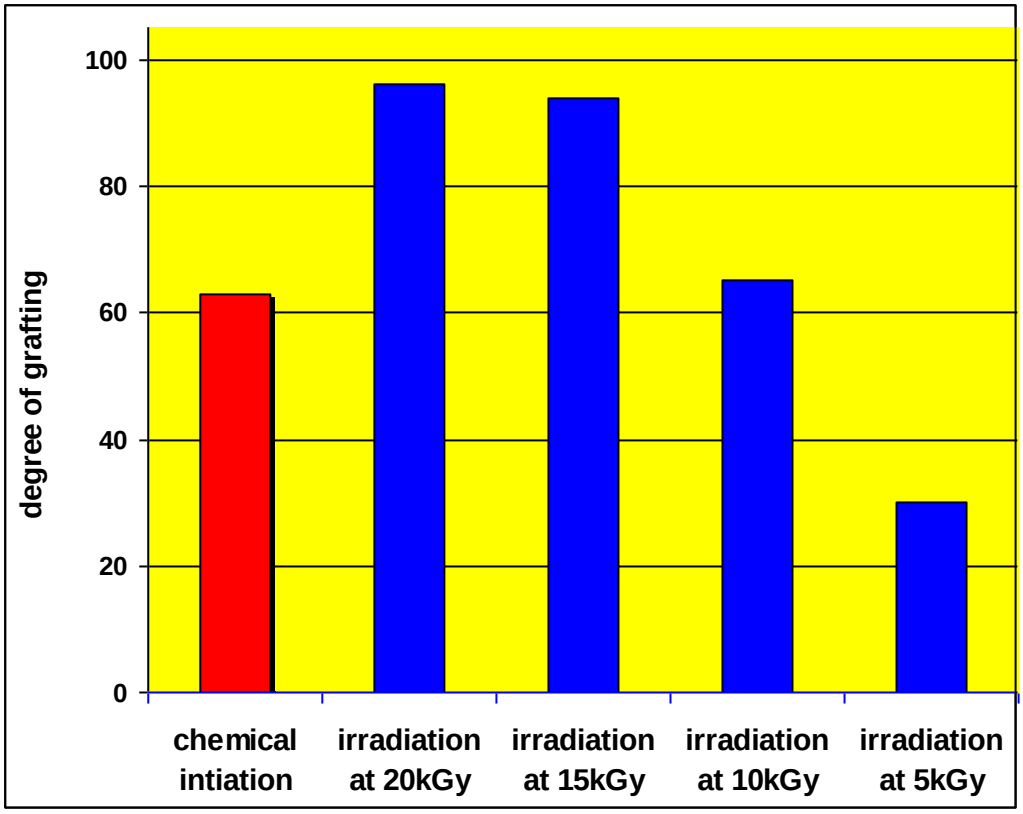

Fig (3.4): Comparison between grafting degree for chemical initiation and irradiation at radiation doses 20, 15, 10, 5 kGy

Further, radiation grafting polymerization is more favorable for the following reasons;

1-Ionizing radiation initiates radical polymerization at ambient temperature in the absence of chemical initiators [155,156]

2-The initiation step of radiation polymerization is temperature-independent, and the overall activation energies are much smaller than in the chemically initiated process [157-159]

And moreover, the advantage of using radiation–induced polymerization is that the polymer is

i- Homogeneous

ii- Free from any impurities

iii-The molecular weight of the formed polymer is controlled by varying doses and dose rates.

3.1.1.4 Conversion of nitrile polymer to amidoxime sorbent.

Chelating properties of the grafted starch can be achieved by conversion of the reactive intermediates, nitrile groups, into chelating amidoxime groups by chemical treatment with hydroxyl amine solution. The grafted polymer was then extensively washed to remove the homopolymer and the unreacted monomer, and then dried. Conversion of the nitrile polymer to the amidoxime sorbent was carried out by reacting the polymer with hydroxylamine according to the following reaction;

Conversion of nitrile to amidoxime:

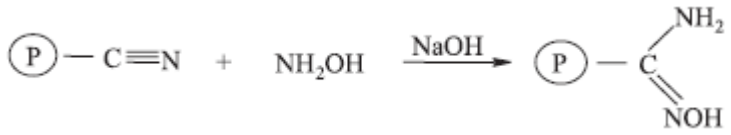

(5)

This was performed by refluxing the nitrile polymer with hydroxylamine at 70 C^0 for 2 h as given in the experimental. After washing and drying at 50 C^0 to constant weight, the sorbent is then ready for characterization.

3.1.1.5 Characterization of amidoxime chelating starch sorbent

The amidoxime chelating starch sorbent was characterized in terms of the starting materials (Starch and PAN) and the final product. These materials were investigated using elemental analysis, particle size distribution, surface area, IR spectrum, thermo-gravimetric analysis and morphology.

i- Elemental chemical analysis :

Elemental analysis of the used starch, the polynitrile polymer and the prepared amidooxime sorbent are given in Table (3.1). High content of nitrogen in the polynitrile polymer and the amidoxime sorbent indicate the good grafting of these materials. The elemental analysis spectra for the original starch, PAN grafted, amidoxime as given in Fig (3.5). The amount of oxygen was determined by difference.

Table (3.1): Elemental analysis for the original starch, PAN grafted, amidoxime.

Element	Starch	Polyacrylonitrile	Amidoxime
N	0.14	17.9	18.1
C	41.7	63.8	36.8
H	6.52	5.86	5.42
O	51.65	12.44	39.68

1- Starch

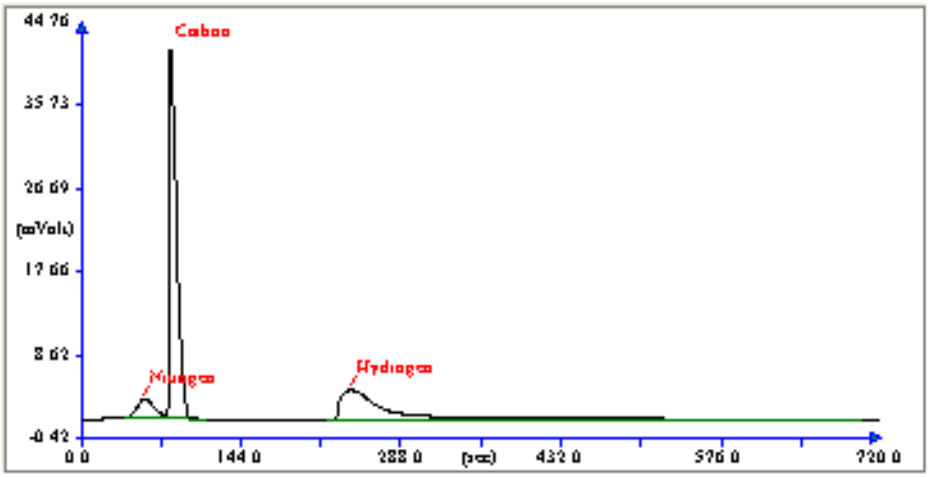

2- Polyacrylonitrile

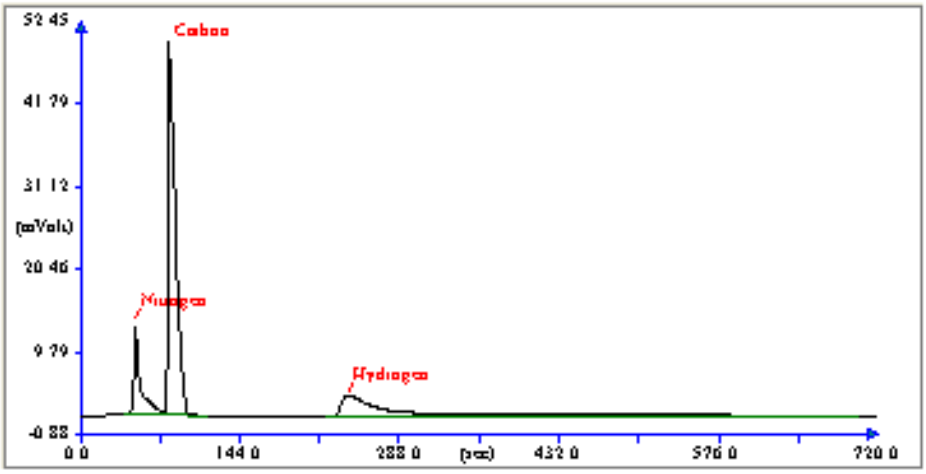

3- Amidoxime

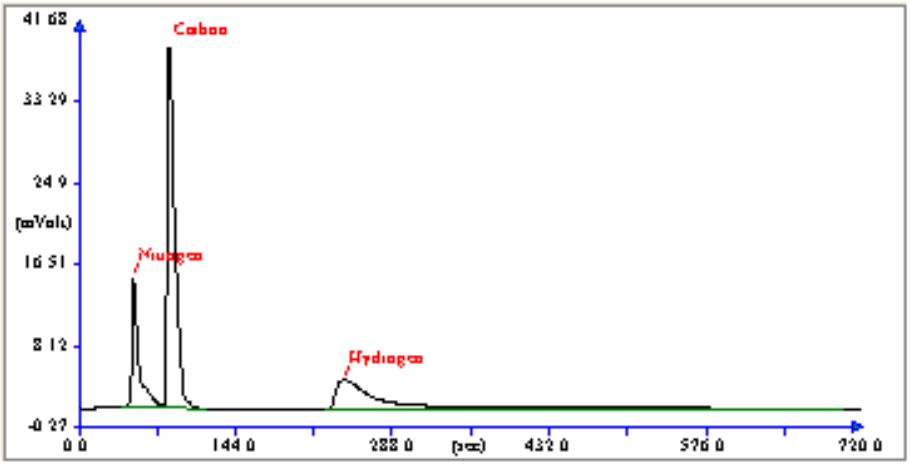

Fig (3.5): The elemental analysis spectra of (C, N, H) for the original starch, PAN grafted, amidoxime

It is of interest to notice that the prepared amidoxime sorbent contain 18.1 % nitrogen and 39.68% oxygen. Correlation these results to mole fraction, it is found that in the amidoxine sorbent 1.29 mole of nitrogen is associated with 2.48 mole of oxygen. That it to say, that each mole of nitrogen corresponds to 2 mole of oxygen to form the amidoxime function group of the prepared sorbent.

ii- Particle size distribution :

Particle size distribution of the fine particles play essential roles in the characterization of the synthesized powder. Due to the synthesis process of chelation there are differences in particle size distribution for starch, polyacrylonitrile, and amidoxime as shown in Fig (3.6) and in Table (3.2). For good measurements we must know the statistical mean of the tool of for the measurable data and must measure of the central tendency in terms of the mean, the median and the mode.

Table (3.2): Particle size distribution, arithmetic statistics for the synthetic materials (starch, Polyacrylonitrile, and Amidoxime) using sedigraph 5100.

Samples	**Median***	**Mean****	**Mode*****
Starch	**10.8** ±0.5 µm	**11.1** ±0.5 µm	**10.6** ±0.5 µm
Polyacrylonitrile	**70** ±3 µm	**85** ±3 µm	**67** ±3 µm
Amidoxime	**90** ±4 µm	**52** ±2 µm	**45** ±2 µm

*The median: The value which divides a series of ordered observations so that the number of items above it is equal to the number below it.

**The mean: The sum of the observations divided by the number of observations.

***The mode: The value that occurs with the greatest frequency. This is used when a quick and approximate measure of the central tendency is desired.

A --- starch (Median = 10.84 µm)

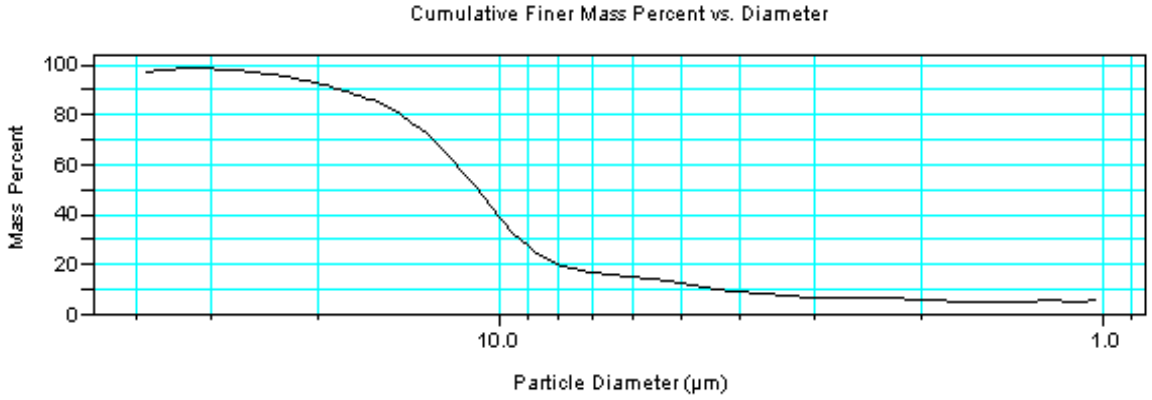

B --- polyacrylonitrile (Median = 69.69 µm)

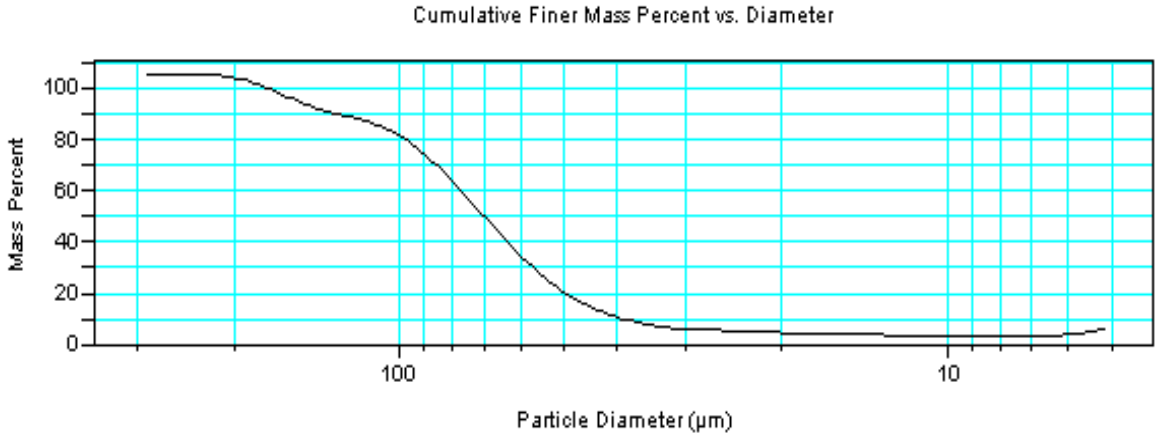

C ---Amidoxime (Median = 90.2 µm)

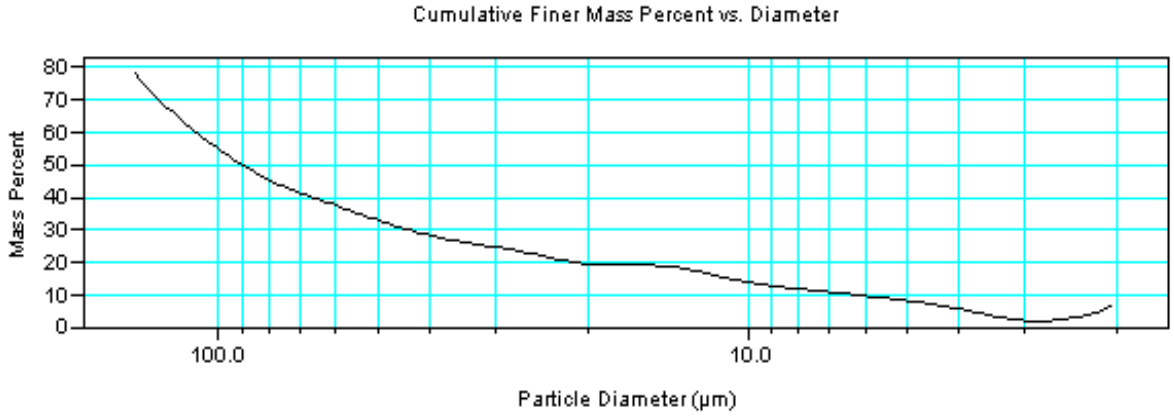

Fig (3.6): Particle size distribution for starch, polyacrylonitrile and amidoxime using sedigraph 5100

iii- Surface area

The adsorption properties of amidoxime depend principally on its inner surface area. The specific surface area is usually derived from the nitrogen adsorption isotherm. The starting point in estimating the specific surface area is the adsorption isotherm. The adsorption isotherm of nitrogen at 77 K is presented in Fig.(3.7) and Table(3.3) for starch, polyacrylonitrile, and amidoxime. The isotherm is Type I, on which monolayer adsorption can occur. Its very important to degassing of the samples before the measurement of the surface area of the samples, to remove any adsorbed gas in the surface of the samples before the measurement. The degassing process is temperature dependent as shown in Fig (3.8). The effect of temp of degassing on the surface area measurement of starch as starting material for synthesis of chelating amidoxime is very important and from the figure it is clear that the best degassing temp for surface area analysis of starch is 210 ^{0}C and after this temperature the materials of starch will be destroyed or broken and the surface area will be lower than the accurate value. The improvement in the surface area due to the synthesis processes, for starch, polyacrylonitrile, and amidoxime are presented in Fig (3.9) and Table (3.4).

Table (3.3): Adsorption isotherms of starch, polyacrylonitrile, and amidoxime.

Relative pressure	Vol. Adsorbed by **starch**(cc/g STP)	Vol. Adsorbed by **acrylonitril** (cc/g STP)	Vol. Adsorbed by **amidoxime**(cc/g STP)
0.0499	0.092	2.143	1.619
0.0874	0.110	2.395	1.844
0.1249	0.124	2.638	1.996
0.1624	0.136	2.778	2.118
0.1998	0.148	2.955	2.226

Table (3.4): Surface area reports for the synthetic samples

Sample	BET Multipoint surface area	BET Single point surface area	Langmuir surface area
Starch	0.570 m^2/g	0.517 m^2/g	0.810 m^2/g
Acrylonitrile	10.758 m^2/g	9.958 m^2/g	12.895 m^2/g
Amidoxime	8.108 m^2/g	7.747 m^2/g	11.083 m^2/g

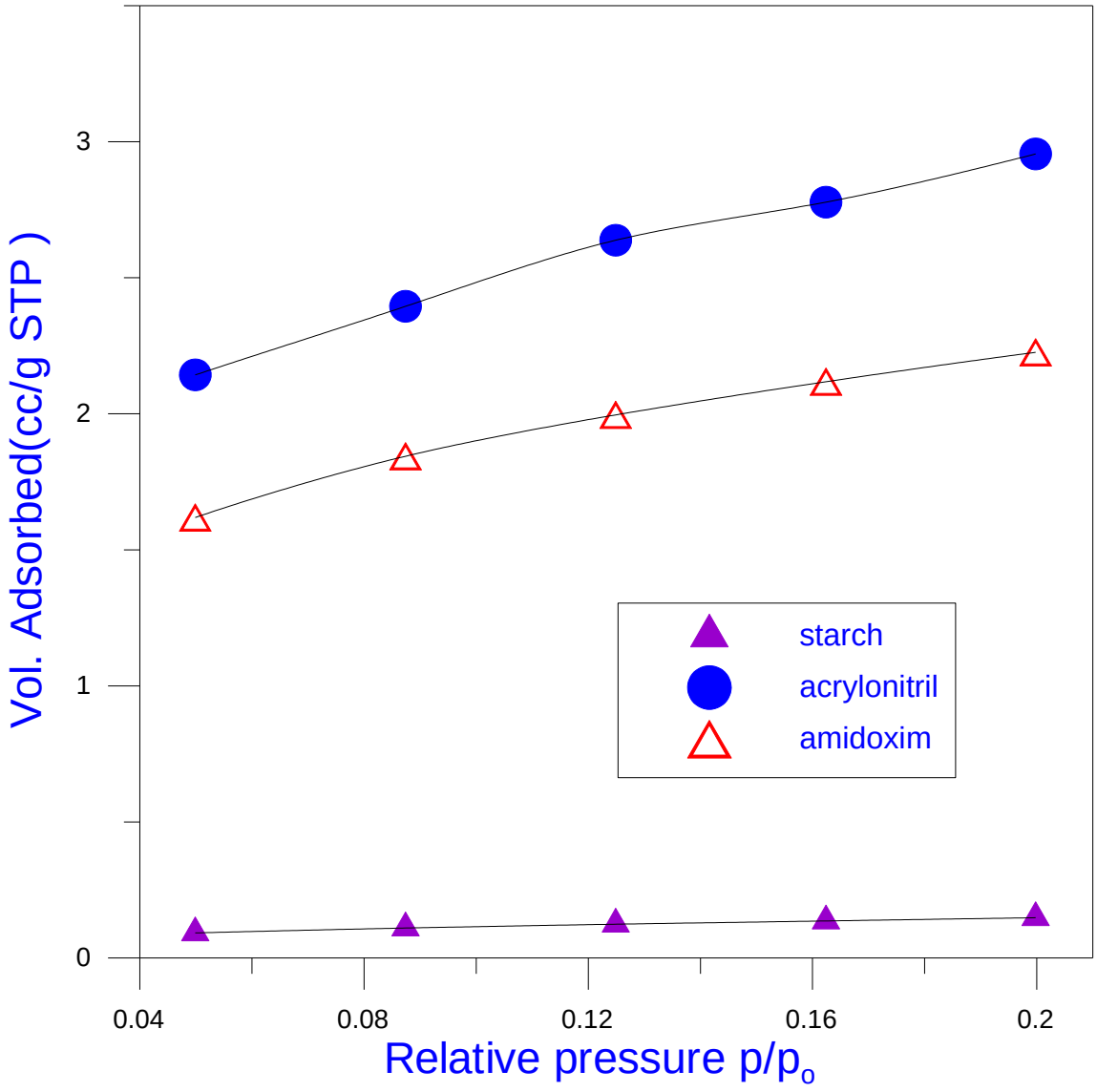

Fig (3.7): The adsorption isotherm of N_2 at 77K for starch, polyacrylonitrile, and Amidoxime sorbent.

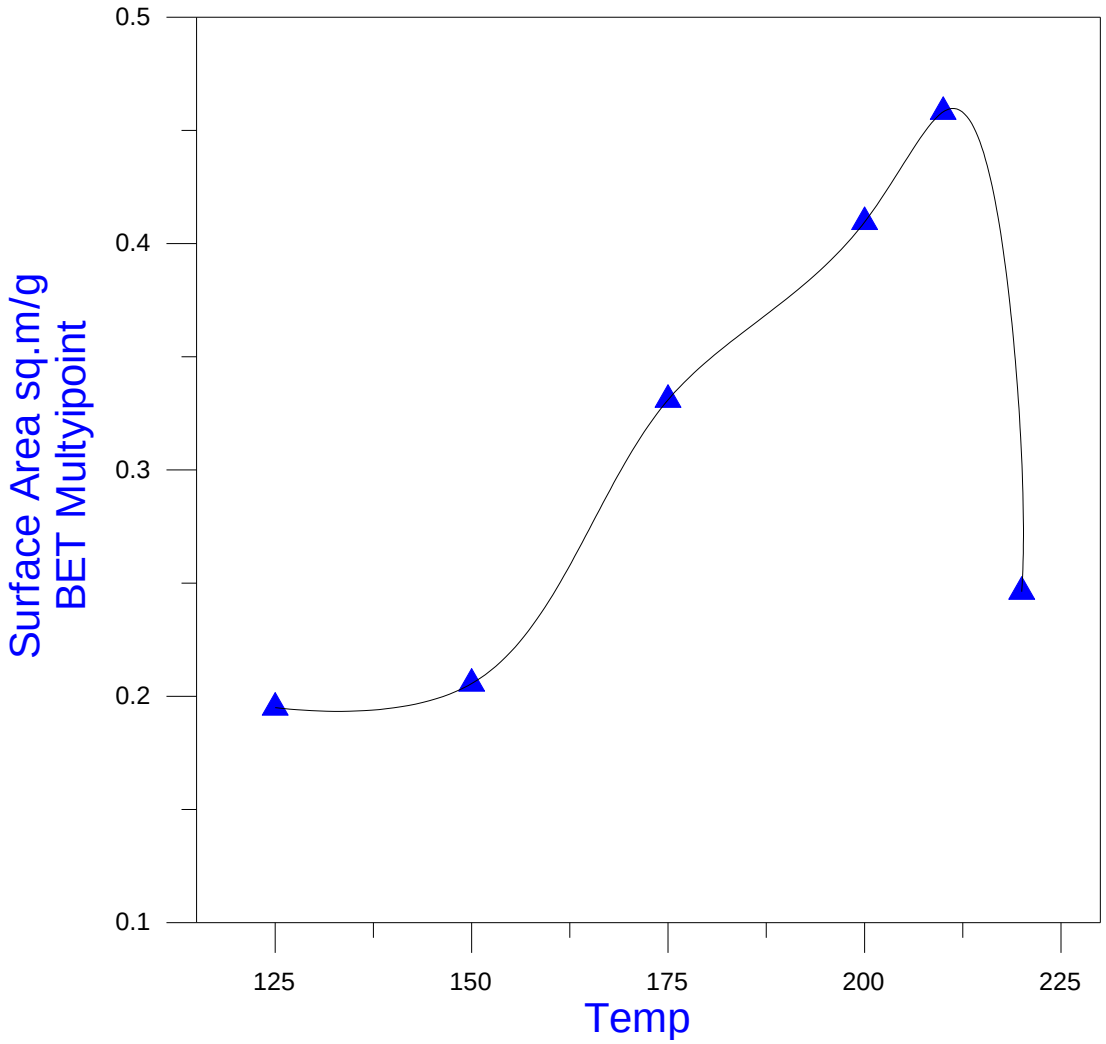

Fig (3.8): The effect of temp of degassing on the sample preparation for the surface area measurement for starch.

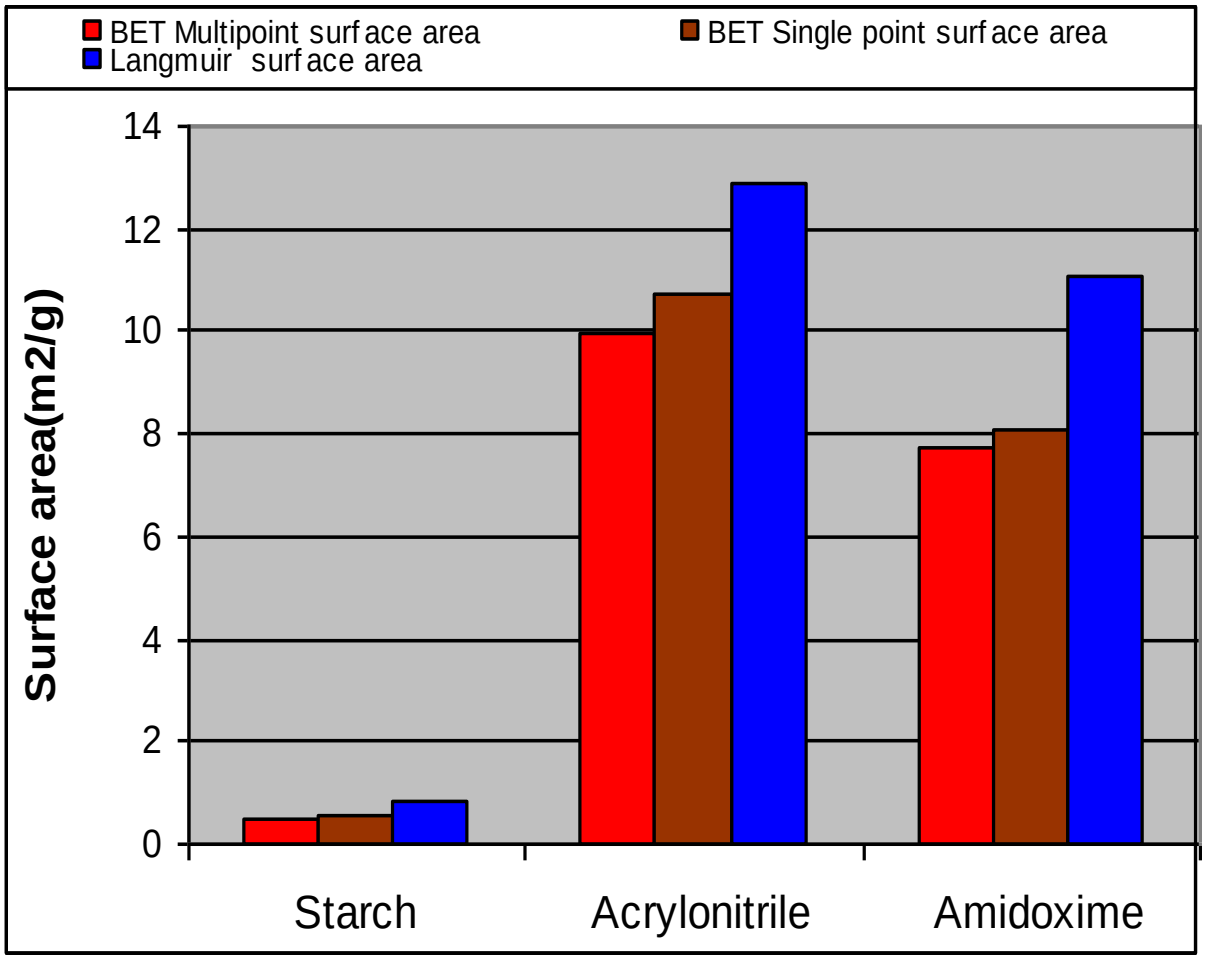

Fig (3.9): Effect of synthesis processes on the surface area of each material using Gemini 2360.

It is clear that the grafted polynitrile product has the highest surface area and starch the smallest. On the other hand, when reacting the grafted polynitrile materials with hydroxylamine, to produce the amidoxime sorbent the surface area decreases. Further, the surface area measured by the BET multipoint technique is slightly higher than that measured by the BET single point method. In all cases, the Langmuir surface areas are higher than that measured by BET.

iv- Analysis of FT-IR spectra

The FT-IR spectra of wheat starch, polyacrylonitrile grafted wheat starch, and the amidoxime resin were investigated. The FT-IR spectrum of the wheat starch showed characteristic absorption bands at 2393.3 and 1648.7 cm^{-1} due to O-H stretching and bending modes, respectively as shown in Fig.3.10. (a). In addition, other absorption bands of starch appeared at 2929.8 and 1015.4 cm^{-1} are mainly due to the C-H stretching and bending modes, respectively.

FT-IR spectrum of polyacrylonitrile grafted wheat starch is given in Fig.3.10. **(b)**.The characteristic absorption of polyacrylonitrile at 2245.9 cm^{-1} due to C ≡ N stretching modes in addition to other absorption bands mainly related to the sago starch are observed. After resin preparation and formation of the amidoxime group, the C ≡ N band at 2245.9 cm^{-1} disappeared and a new bands of amidoxime appeared at 1654 cm^{-1}, the band of N-H at 1390.1cm^{-1},and the band of N-O at 926.5, respectively are shown in Fig.3.10.(c).

v- Thermogravimetry analysis:

The thermal degradation of poly(amidoxime) resin and polyacrylonitrile (PAN) grafted starch was performed with a heating rate of 10°C min^{-1} in an N_2 atmosphere and the TG curve are presented in Fig(3.11)

The main weight loss of PAN grafted starch and poly(amidoxime) resin occurs between the range of 290-380°C and 200-480°C, respectively. The same weight loss was found (7%) at 200°C of grafted materials and poly(amidoxime) resin. The poly (amidoxime) resin was slightly less stable than PAN grafted starch up to a temperature of 345°C, and again the resin was more stable than PAN grafted starch up to 1000°C. At the final stage, about 30% weight remain in PAN grafted starch, whereas 36% weight remain in poly(amidoxime) resin was observed until 1000 °C.

a-Starch

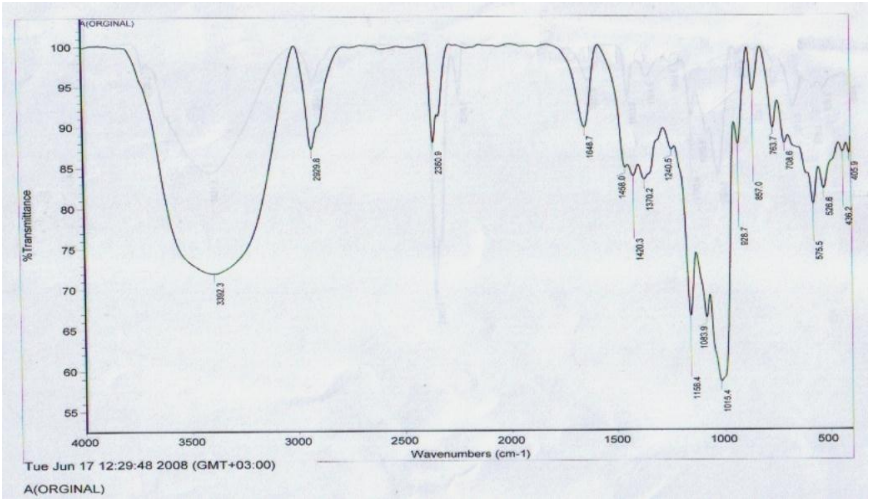

b-PAN

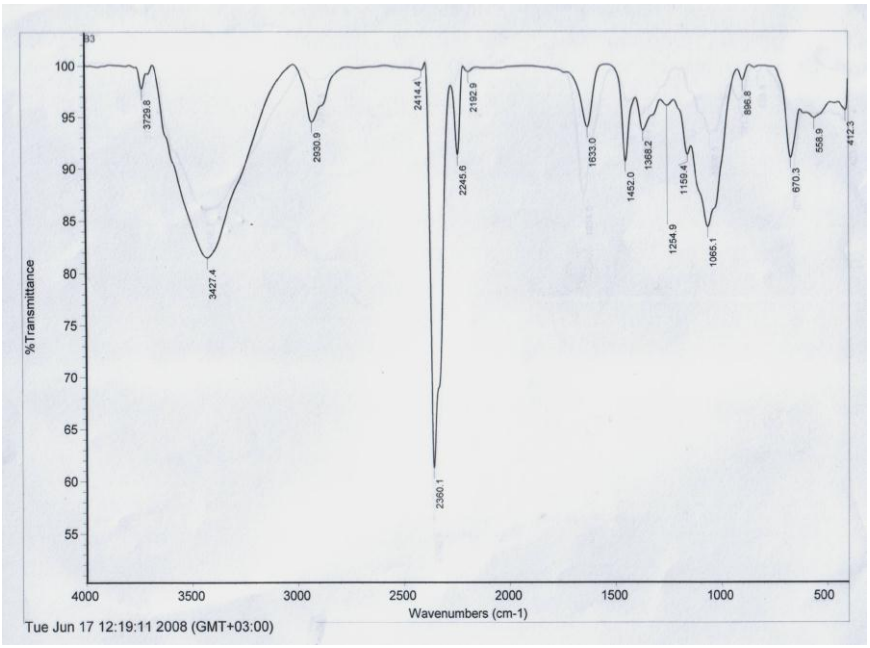

c-Amidoxime

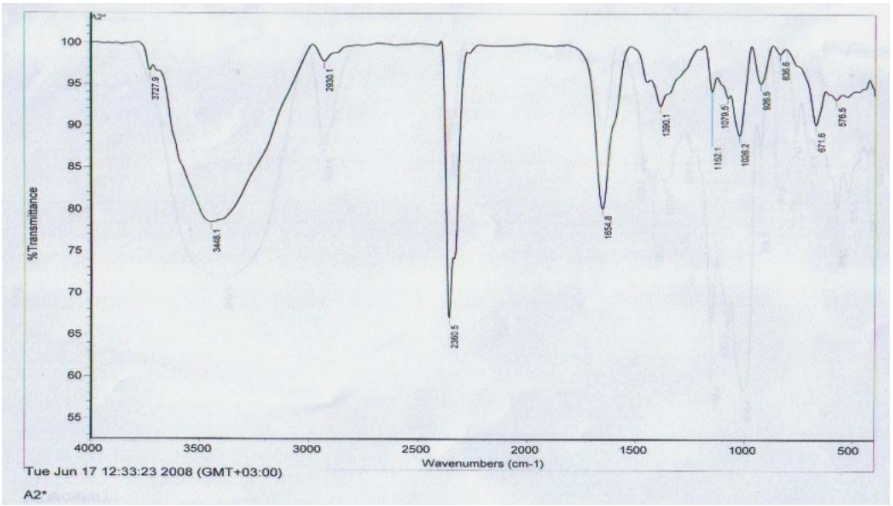

Fig (3.10): FT-IR spectra analysis for starch, PAN induced by irradiation at radiation dose 15 kGy and amidoxime chelating starch.

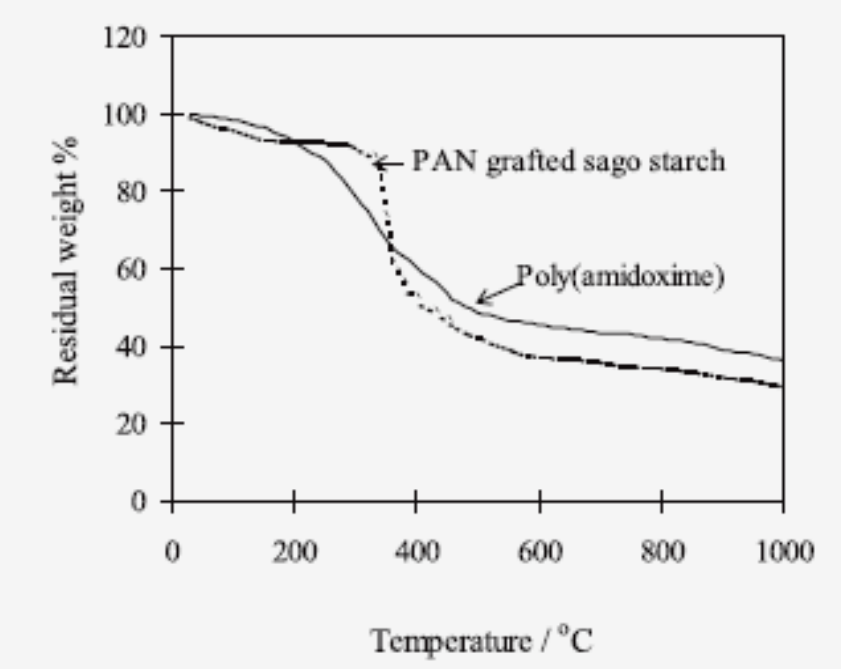

Fig (3.11): The thermo gravimetry analysis of polyacryonitrile grafted, and amidoxime

vi- Morphological Study

It was known that the substitution on the starch backbone destroys some of its properties. The effect of grafting and amidoximation in the fine structure of the starch can be studied using scanning electron microscope (SEM). Figs.(3.12a, b and c) show the SEM photos for the original starch, PAN grafted, and amidoxime, respectively.

a-Starch

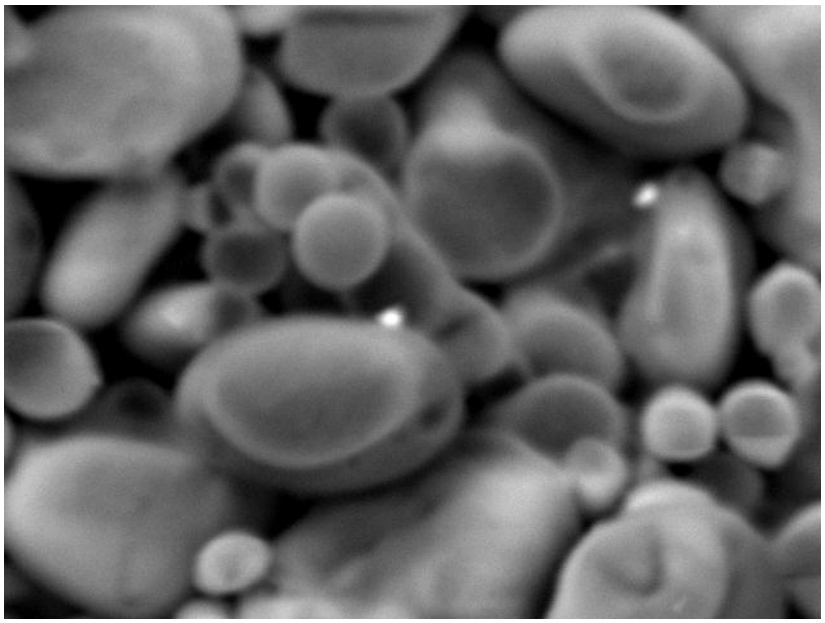

Mag	: x2200
Acc.V	: 15kv
WD	: 20mm
Spot size	: 48

b- Polyacrylonitril

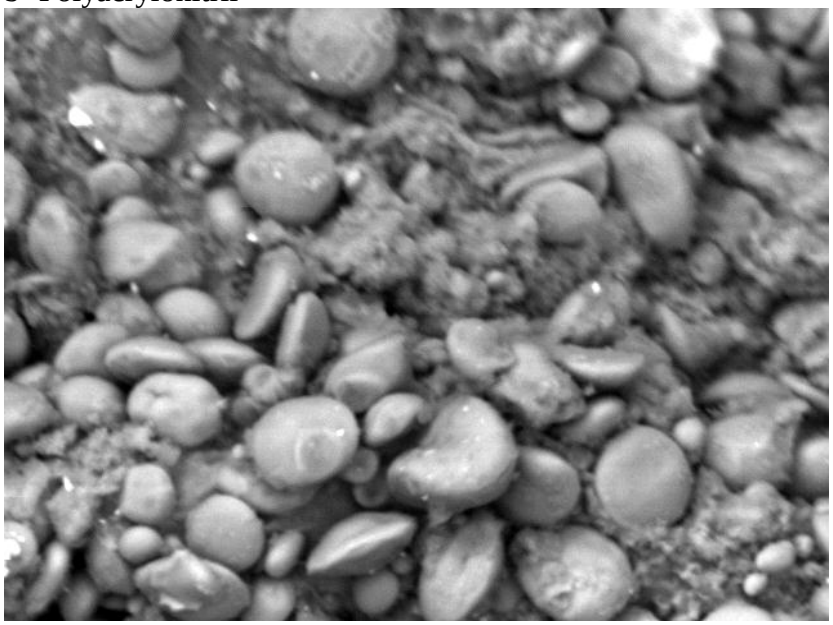

Mag	: x750
Acc.V	: 15kv
WD	: 20mm
Spot size	: 48

Fig (3.12 a and b): SEM photos for the (a)original starch, and (b) PAN grafted, respectively.

c- Amidoxim

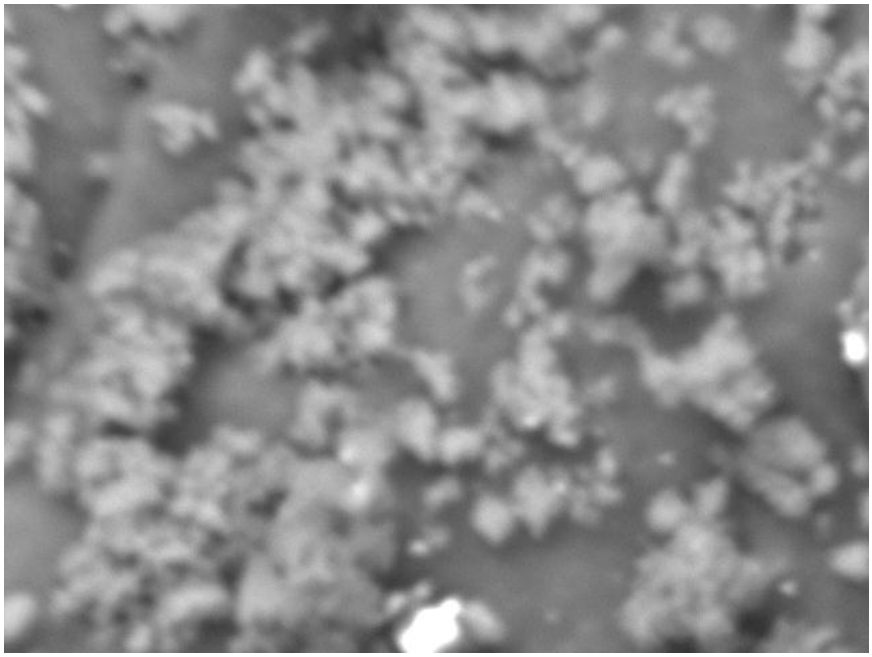

Mag	: x2200
Acc.V	: 15kv
WD	: 20mm
Spot size	: 48

Fig (3.12 c): SEM photos for the (c) amidoxime sorbent.

3.1.2 Preparation of activated carbon

Among many types of adsorbent materials, activated carbons which can be produced from almost any carbonaceous material, are the most widely used. This is mainly due to its large adsorptive capacity and low cost [160,161]. Further, activated carbon some times is selective sorbent and in general has high radiation stability

Activated carbon was prepared from charcoal by chemical activation in this study. The preparation process consisted of zinc chloride impregnation followed by carbonization. The carbonization temperature ranges from 500 to 700 ^{0}C for 1 h,

3.1.2.1 Characterization of activated carbon and charcoal

The activated carbon consists mainly of carbon. The properties of activated carbon depends on the original of the carbonaceous material used and the method of activation. Adsorption properties of the activated carbon can be evaluated based on it is characterization as the following.

i- Particle size distribution

Due to the synthesis process of activated carbon from charcoal, there are a difference in the particle size distribution between activated carbon and charcoal. Different technique such as sedigraph 5100, SEM, and mechanical sieving were used for quality control of particle size. This is to assess the agreement between the different techniques for measurement particle size distribution and evaluate the suitable technique for measurement. The following Table(3.5)and Fig (3.13 a and b) represented the measured particle size for charcoal and AC

Table(3.5): Particle size distribution for charcoal and A.C using different technique.

Sample	SEM	**Sedigraph 5100**	**Sieving**
Charcoal	**662** ±**60** µm	**183** ±9 µm	**>300** µm
A.C	**27**±3 µm	**35** ±2 µm	**< 45** µm

It is clear that in the case of charcoal, the particle size determined by SEM is much higher (662 µm) than that measured by the sedigraph 5100 and sieving. This can be related to possible agglomeration of charcoal in case of SEM measurements.

In case of activated carbon, the particle size distribution is more or less within the same rang using different techniques. This come to the conclusion that a simple sieving of AC can gives a good indication of the AC particle size

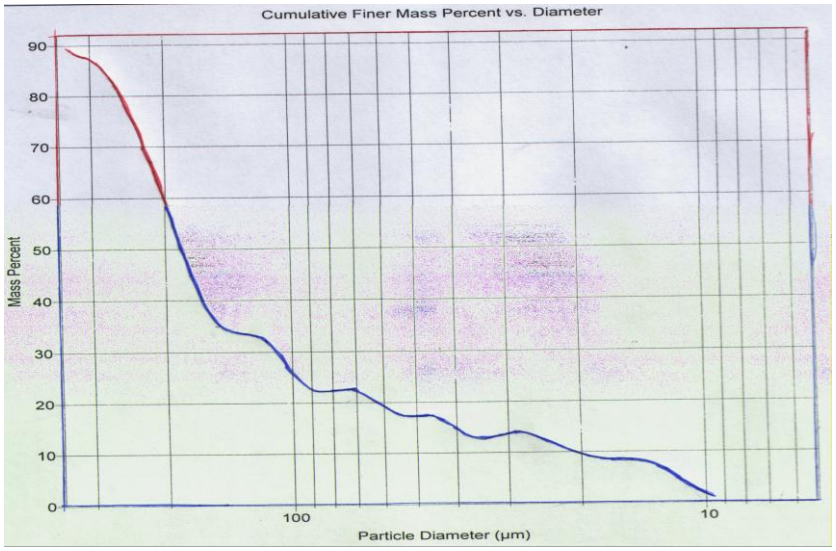

A- Median diameter of Charcoal = 183 µm using sedigraph 5100

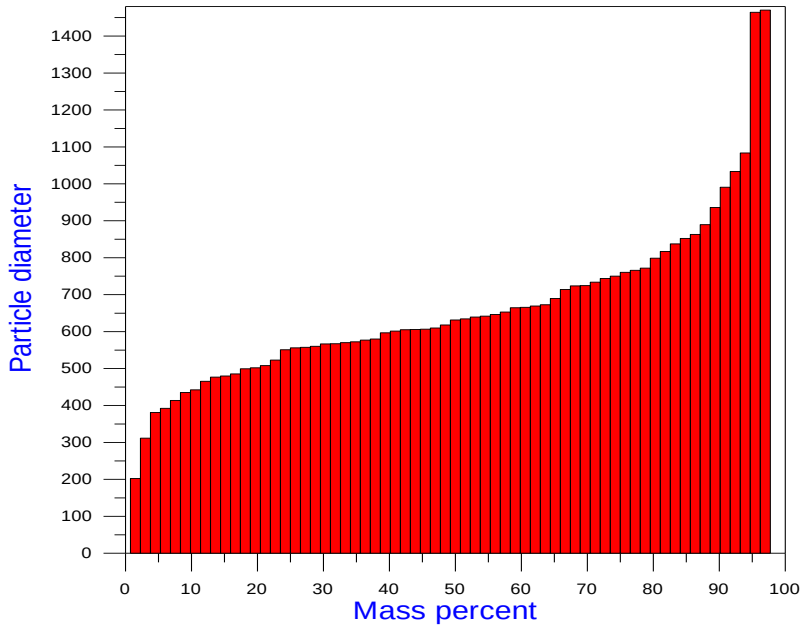

B- Mean of the charcoal = 662 µm using SEM

Fig(3.13A): Particle size distribution, arithmetic statistics for charcoal using Sedigraph 5100, and SEM

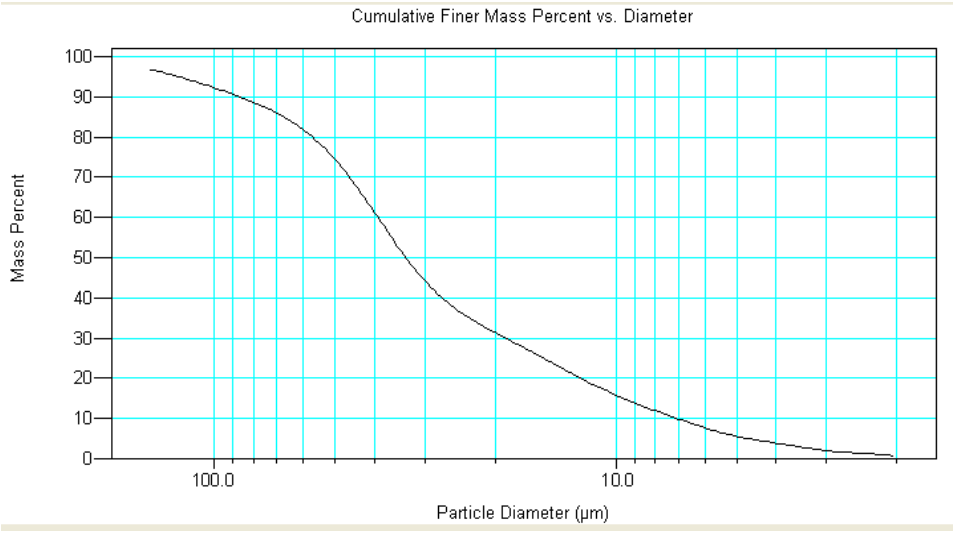

A- Median diameter of A.C = 34.476 µm using sedigraph 5100

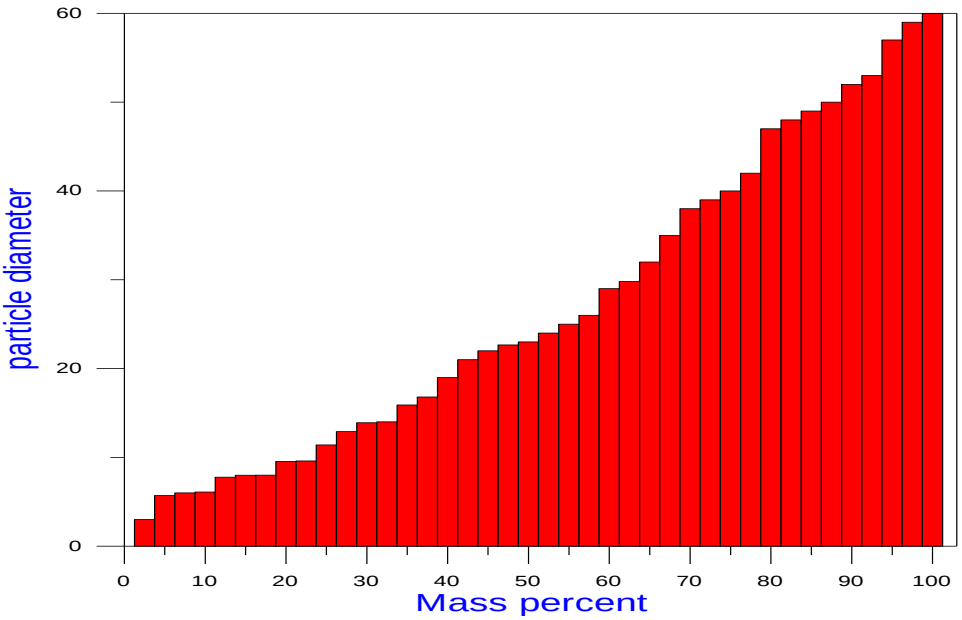

B- Mean diameter of A.C =27.28 µm using SEM

Fig(3.13B): The particle size distribution, arithmetic statistics for A.C using Sedigraph 5100, and SEM

ii- Surface Area

The adsorption properties of activated carbon depend principally on its inner surface area. Activated carbon is often characterized by its pore volume. The starting point in estimating the specific surface area is the adsorption isotherm [162]. The adsorption isotherms of nitrogen at 77 K for charcoal and the prepared AC is presented in Table (3.6) and Fig.(3.14).

The isotherm is Type I, this isotherm is characterized by a plateau which is nearly or quite horizontal. It is typical for microporous adsorbents on which monolayer adsorption can occur.

Table (3.6): Adsorption isotherms for charcoal and activated carbon

Sample	Relative Pressure	Vol . Adsorbed cc / g STP
Charcoal	**0.050** **0.087** **0.125** **0.162** **0.200**	**1.12** **1.25** **1.36** **1.45** **1.53**
Activated carbon	**0.050** **0.112** **0.175** **0.237** **0.300**	**152.1** **169.4** **178.2** **185.2** **190.6**

Based on the isotherms obtained, the values of BET surface area were calculated for charcoal and AC, and given in the Table (3.7).

Table (3.7**):** Surface area of activated carbon and charcoal

Sample	BET Multipoint Surface Area sq. m^2/g	BET Singlepoint Surface Area sq. m^2/g	Langmuir Surface Area sq. m^2/g
Charcoal	5.58	5.34	7.64
Activated carbon	581.2	580.5	876.1

From table 3.7 the surface area of used charcoal is rather small. In this concern the values obtained are 5.58, 5.34 and 7.64 m^2/g as measured by BET multipoint technique, BET singlepoint technique and Langmuir method, respectively. Activation of charcoal with $ZnCl_2$ produced activated carbon with almost more than 100 times much higher than the surface area for the charcoal, and their higher sorption efficiency is expected

(a) Adsorption isotherm for activated carbon

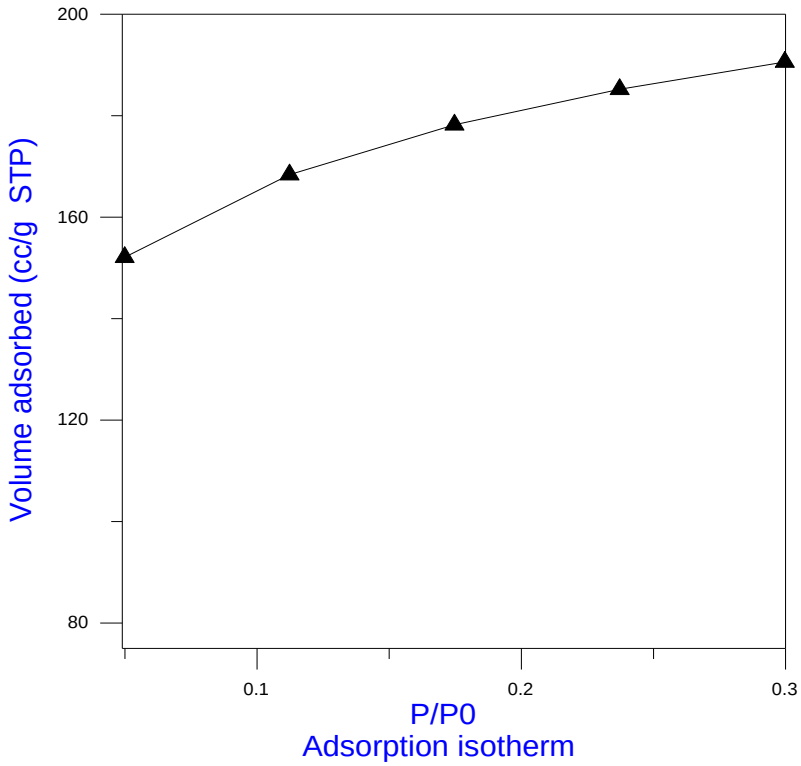

(b) Adsorption isotherm for charcoal

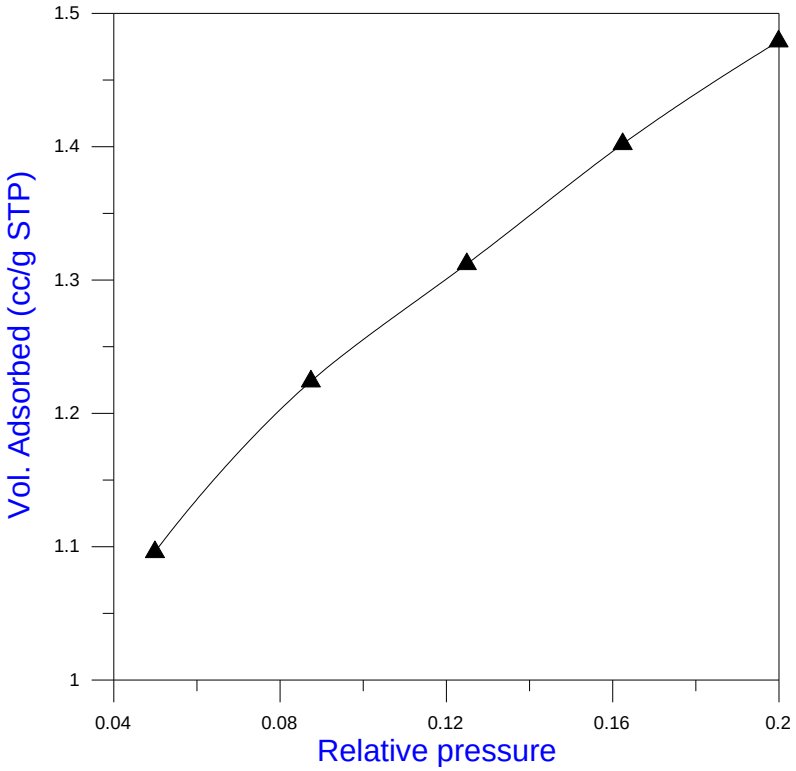

Fig(3.14): Adsorption isotherm of N_2 for (a) activated carbon and (b) charcoal

iii- Morphological Study

The effect of chemical activation on the structure of the charcoal was studied using scanning electron microscope (SEM). Figs.(3.15a and b) show the SEM photos for the charcoal and activated carbon. From these figures, it is clear that charcoal is present as slightly porous granular. On the other hand, AC, is much smaller granular with a more porous nature than charcoal. This morphology is parallel to the data obtained from particle size as well as the surface area measurement and obtained in the previous session.

(a) Charcoal

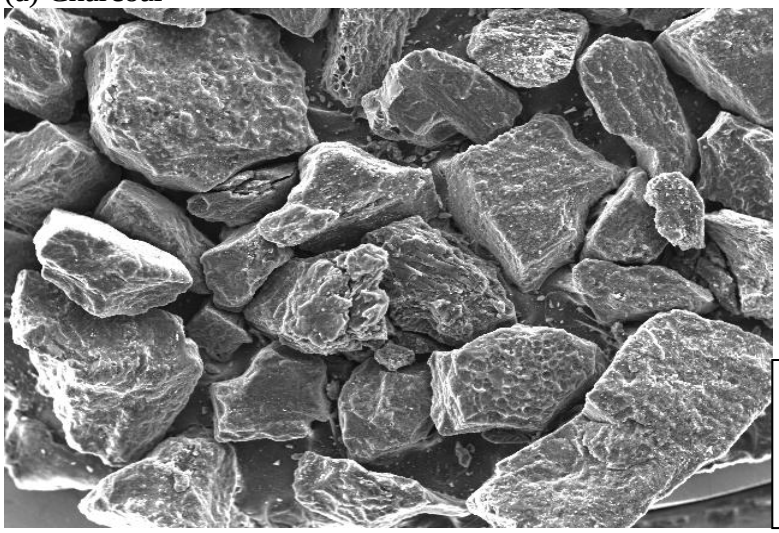

Mga : x35
Acc.V : 30kv
WD : 20mm
Spot size : 36

(b)Activated carbon

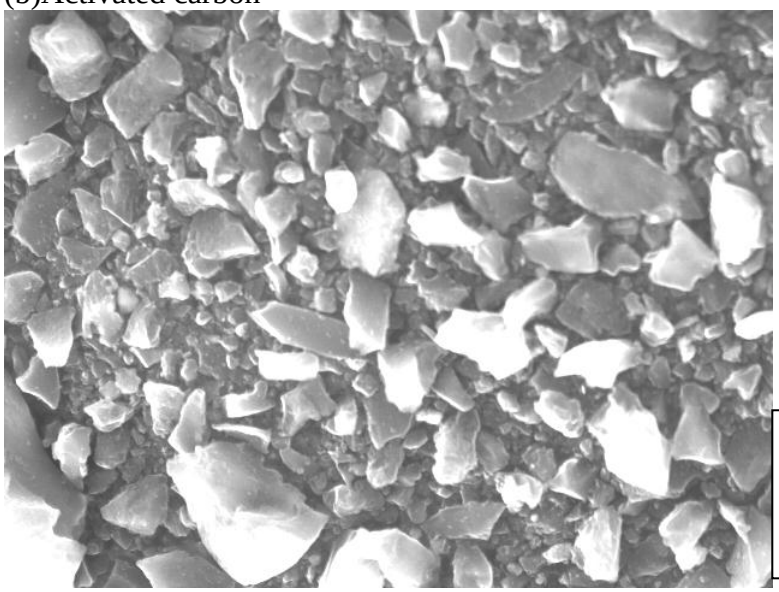

Mga : x2200
Acc.V : 30kv
WD : 8mm
Spot size : 36

Fig (3.15 and b): SEM photos for the charcoal, and activated carbon.

3.2. Sorption of Uranium by the Prepared Sorbents

3.2.1. Sorption on amidoxime chelating starch resin.

The experiments were done to investigate the removal of heavy metals ions especially (uranium) in the waste solution. All experiments were carried out under the following conditions; 50 ml of metals ion solution, agitation rate 200 rpm and the solution temperature was 30 ^{0}C using 0.1 gm of amidoxime resin having particle size of 50-100 µm.

Preliminary investigation were carried out to assess the analytical method recommended for analysis in this investigation. In this respect, uranium content in different batches of waste produced from Egyptian Fuel Manufacturing Pilot Plant were analyzed by ICP-AES and UV-Visible Spectrophotometer

Uranium content in the waste of mother liquor of FMPP were determined by ICP-AES and UV-Visible using Arsenazo, to verify and assure the required specifications of uranium content. As shown in Fig (3.16) and Table (3.8) there are high agreement between the two results. Accordingly, UV-Visible Spectrophotometer was used for uranium determination for sorption investigation.

Table (3.8): Uranium content in waste mother liquor (different batches) using ICP-AES and UV-visible

Batch number*	U content using ICP-AES	U content using U.V-Visible
SML/044/08	8.7 ppm	9.2 ppm
SML/045/08	11.5 ppm	12.0 ppm
SML/046/08	19.1 ppm	20.2 ppm
SML/047/08	9.4 ppm	9.3 ppm
SML/048/08	9.549 ppm	10.18 ppm

Batch number*: mother liquor samples from FMPP uranium waste

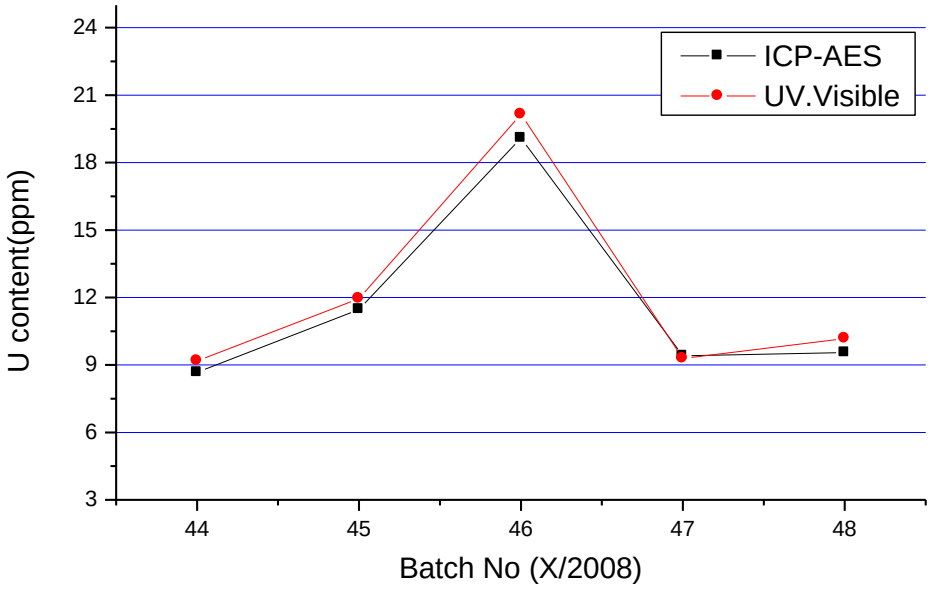

Fig (3.16): The comparison between ICP-AES and UV-Visible Spectrophotometer for analysis of uranium for mother liquor samples from FMPP

i- Effect of hydrogen ion concentration, pH.

Hydrogen ion concentration is an important factor affecting on the recovery of U(VI) from waste of FMPP by the amidoxime sorbent. The influence of pH value on the adsorption of U(VI) towards the prepared polymeric adsorbent containing amidoxime chelating functional group was investigated. The percent removal of uranium as a function of pH, using uranium concentrations of 100 mg/l, a resin weight of 0.1g, and shaking time 3 hr is shown in Fig.(3.17). It is clear that the adsorption of U(VI) strongly dependent on the hydrogen ion concentration in the aqueous phase. U(VI) showed low adsorption in the pH range of 2.0 to 3.0. The adsorption of U(VI) increased significantly from pH 4.0 to 6.5 and then decreased evidently at pH 7.0 . As the pH value increased to 7.5 and especially greater than pH 8.0, the % removal of U(VI) decreased. It is noticed that at pH 8 and higher, colloid U(VI) formation was observed which is reflected on the decrease of the amount of % removal. Therefore, to obtain the highest uranium removal using the prepared amidoxime sorbent the medium pH is adjusted to 6.5 .

ii- Effect of shaking time.

Figure(3.18) indicate that removal efficiency increased with an increase in contact time before equilibrium is reached**.** The optimal contact time to attain equilibrium with amidoxime resin was experimentally found to be about 60 min.

It has been observed that [163] the mechanism of metal removal from the aqueous metal involved four steps:

(i) migration of metal ions from the bulk solution to the surface of the adsorbent;

(ii) diffusion through boundary layer to amidoxime surface;

(iii) adsorption at a binding site

(iv) intra particle diffusion into the interior of the resine.

The boundary layer resistance will be affected by the rate of sorption and increasing the agitation time will reduce this resistance and increase the mobility of the ions. However, because the process is time dependent, after about 60 min, of agitation, adsorption remains slightly or relatively constant. It is observed that the uranium uptake ratio reaches 50% at 10 min ($t_{1/2}$).

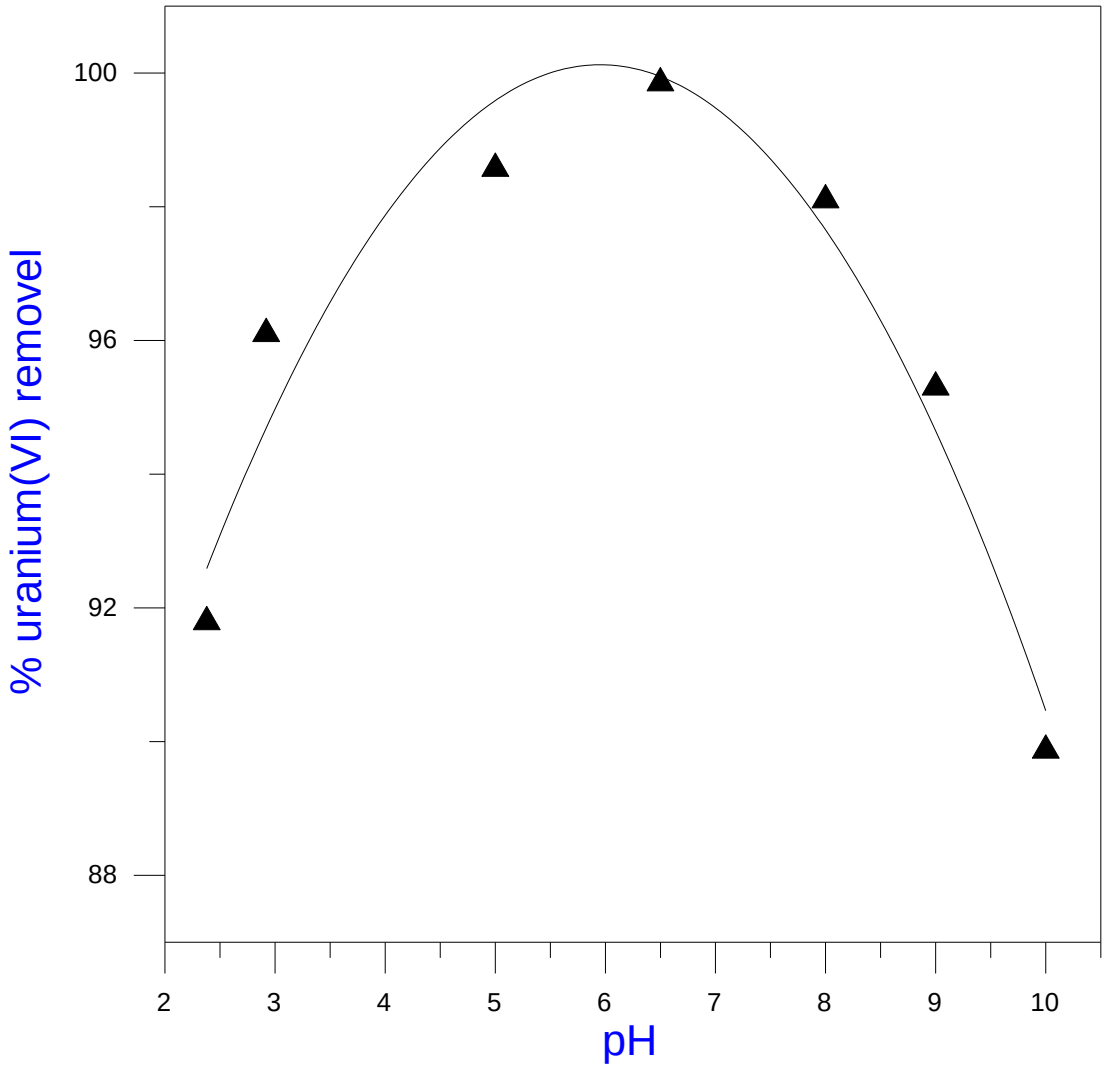

Figure (3.17): Effect of pH on the sorption of uranium by amidoxime resin (resin weight of 0.1g, Uranium concentrations of 100 mg/l , time 180 min)

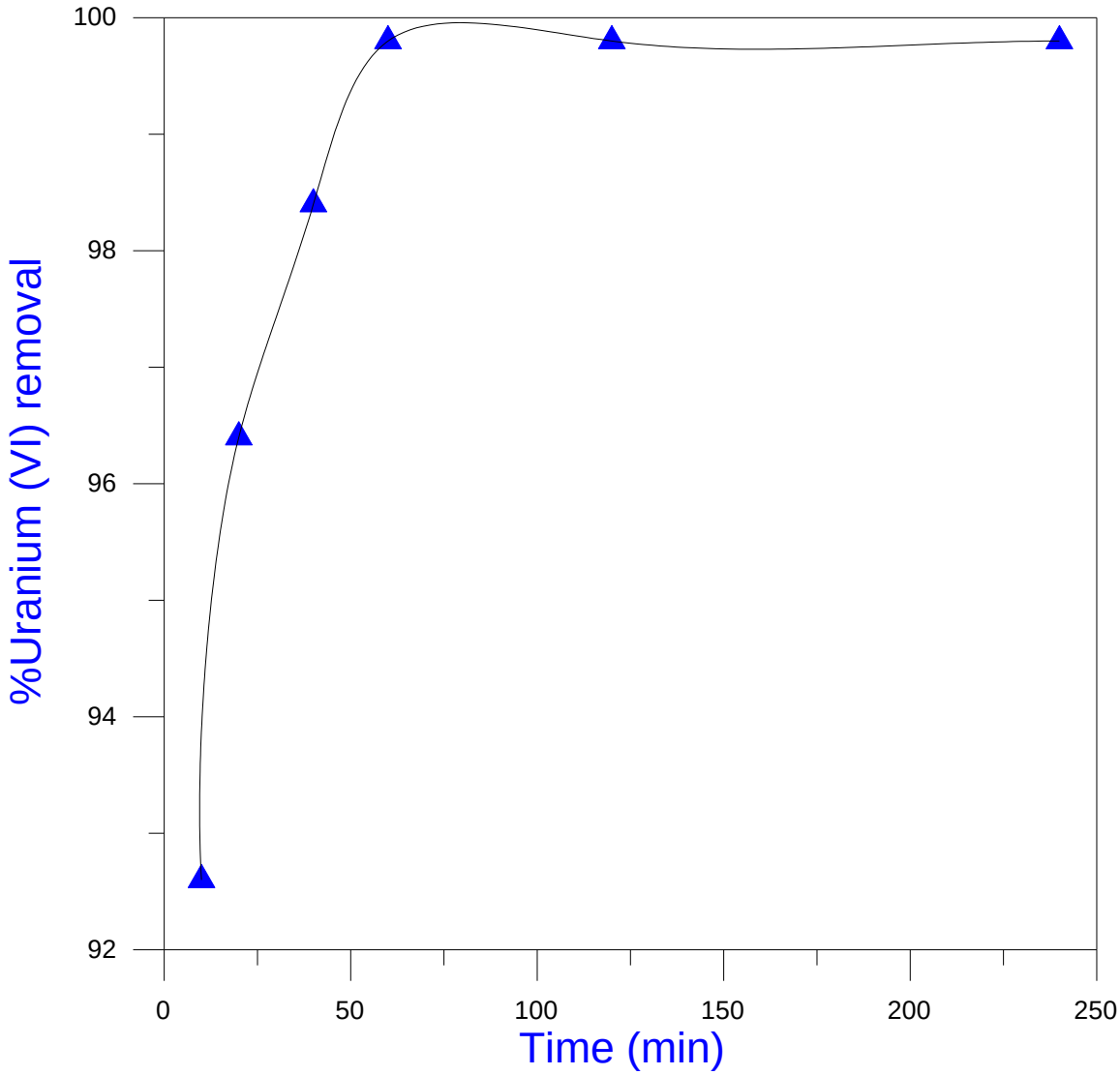

Figure (3.18): Effect of shaken time on the sorption of U by amidoxime sorbent (pH = 6.5, resin weight of 0.1g, Uranium concentrations of 100 mg/l)

iii- Effect of resin weight.

The percentage removal of uranium is found to increase with increasing amidoxime sorbent to reach a maximum uptake of more the 97% as shown in Figure (3.19). Under these condition, the amount of uranium sorbed corresponds to sorption of 4.85 mg uranium per 0.05 g amidoxime sorbent. This corresponds to a sorption capacity of the resin of about 97 mg uranium/g sorbent.

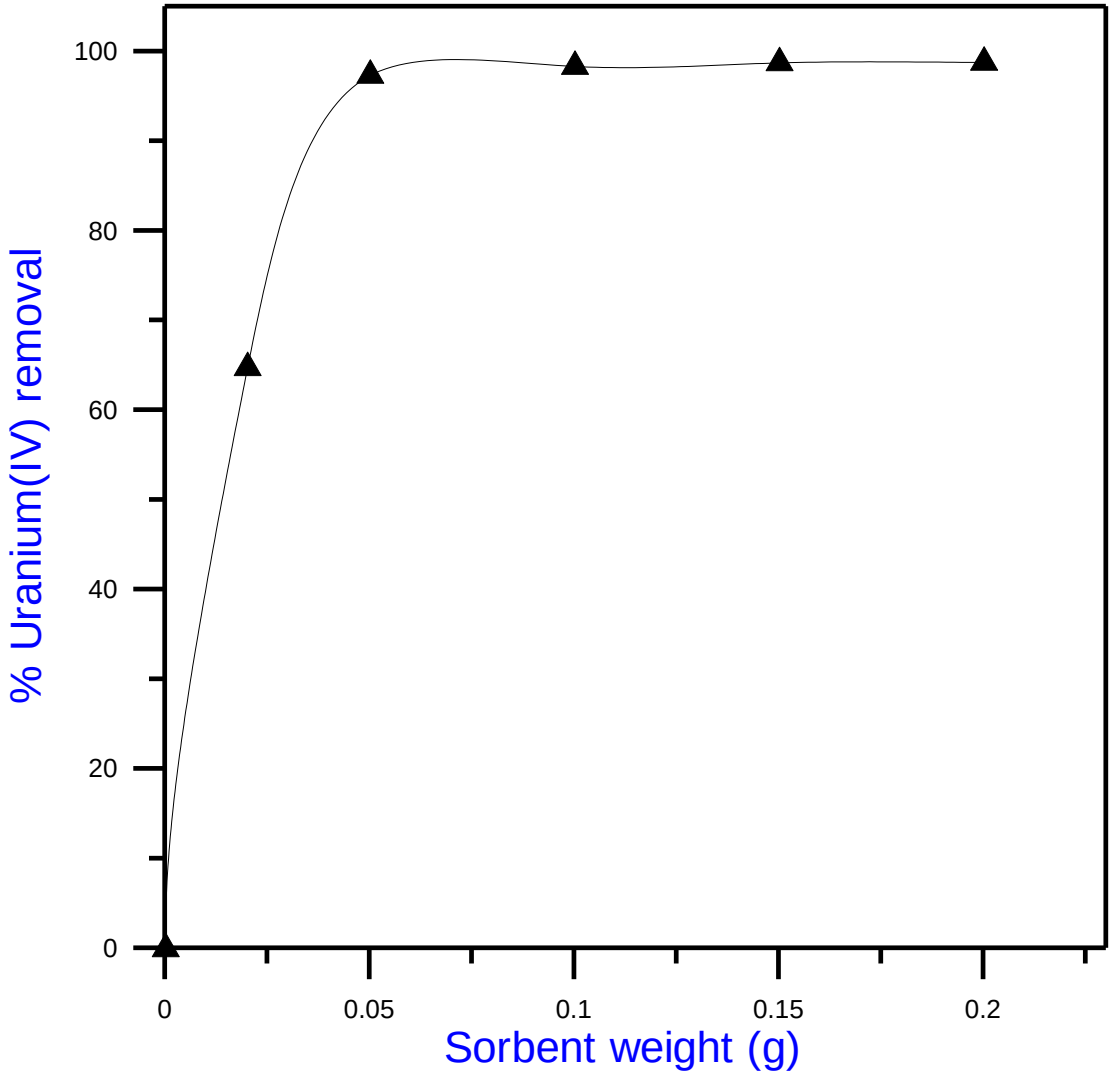

Figure (3.19): Effect of sorbent weight on the sorption of uranium by amidoxime resin (pH = 6.5, Uranium concentrations of 100 mg/l , time 60 min)

iv- Effect of temperature

The effect of temperature on the sorption of uranium is given in figure (3.20). From this figure it is clear that by increasing the temperature the percent removal of uranium increased. This indicates that extraction is endothermic. This could be related to possible dehydration of uranium and thus decrease the competition of uranium hydration in solution and / or the increase in the amidoxime sorbent pore and thus increase the availability of internal site of the sorbent to react with uranium.

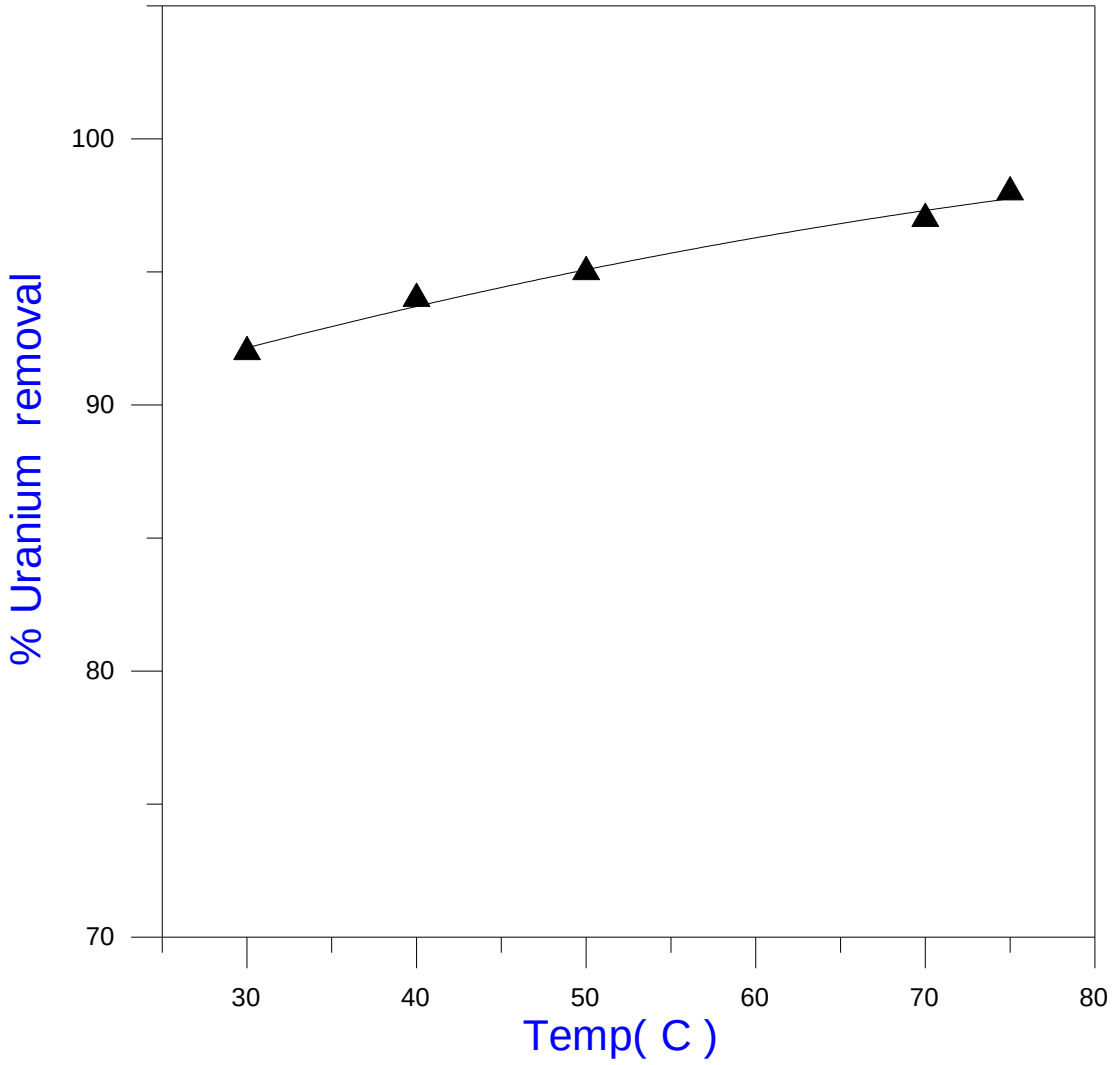

Fig(3.20): Effect of temperature on uranium sorption by amidoxime sorbent **(**pH= 6.5, resin weight of 0.1g, uranium concentrations of 100 mg/l, and time 60 min**)**

v- Effect of initial uranium concentration.

The effect of initial uranium concentration on the percentage removal of uranium by the amidoxime sorbent is shown in Figure (3.21A). It can be seen from the figure that the percentage removal decreases with the increase in initial uranium concentration.

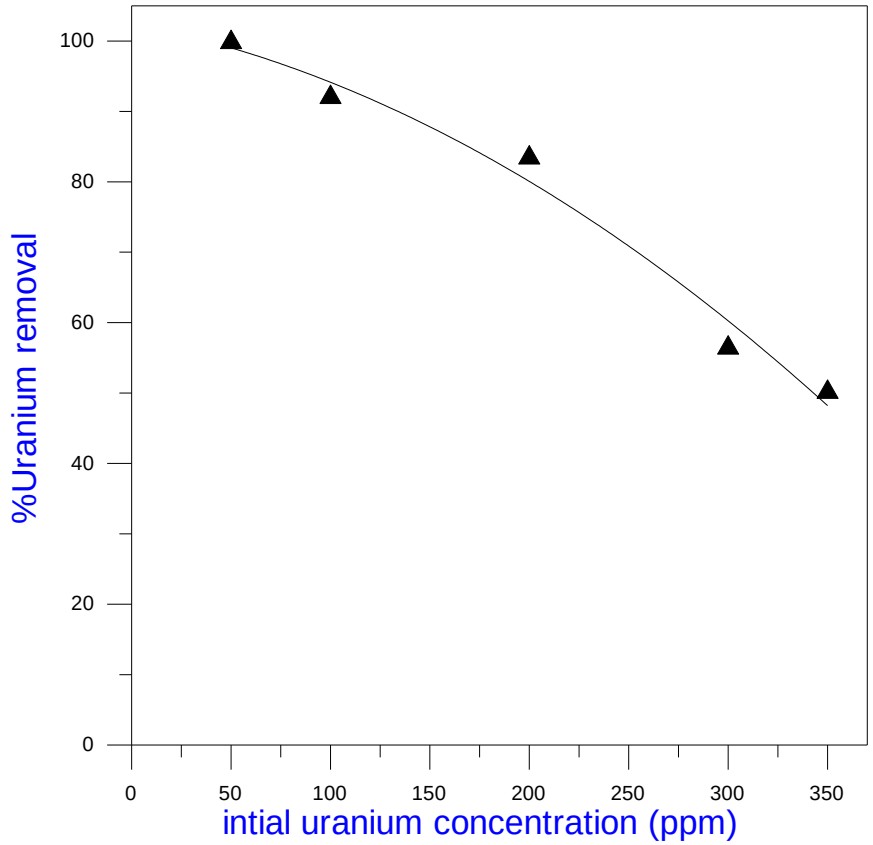

Figure (3.21A): Effect of Variation of the percent adsorption with initial uranium concentration. **(**pH = 6.5, weight of 0.1g, and time 60 min**)**

vi- Adsorption isotherms

The sorption isotherm representing mg/g on the sorbent against the initial uranium concentration in solution is given in figure (3.21B). It is clear that from the figure, the amount of uranium ions adsorbed per unit mass of amidoxime sorbent increases as the initial uranium concentration increase then tend to level off.

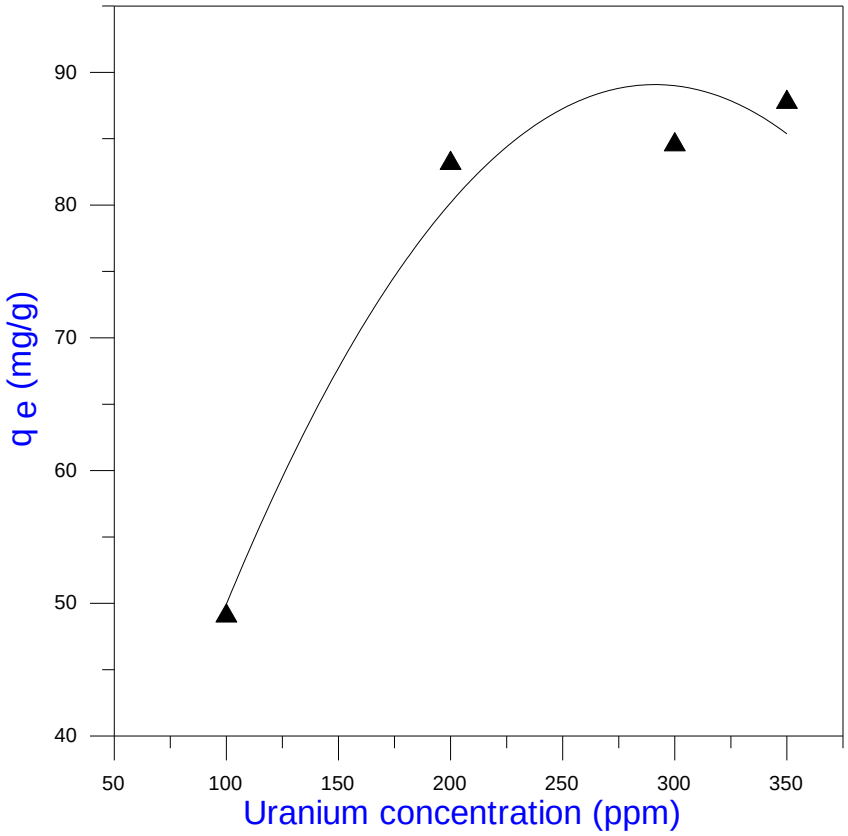

Fig (3.21B): Effect of initial uranium concentration on variation of the amount of uranium ions adsorbed per unit mass of adsorbent **(**pH = 6.5, 0.1g of resin, and shaken time 60 min**)**

The adsorption studies were conducted at fixed initial concentration of heavy metals by varying adsorbent dosage. The equilibrium data obtained were analyzed in the light of Langmuir and Freundlich isotherms as given in the introduction chapter.

Freundlich equation is given by [164].

$$q_e = K_f C_e^{\frac{1}{n}} \quad (8)$$

Taking the logarithmic form of the equation

$$Log(q_e) = Log(K_f) + \frac{1}{n} Log(C_e) \quad (9)$$

Langmuir equation is given by [165].

$$q_e = \frac{abc_e}{(1+bc_e)} \quad (10)$$

The linearized expression of this equation is

$$\frac{1}{q_e} = \frac{1}{a} + \frac{1}{abC_e} \quad (11)$$

This equation is called the "Double-Reciprocal Langmuir Equation" and is more suitable for situations in which the distribution of equilibrium concentrations tends to be skewed towards the lower end of the range of the equilibrium concentrations. where q_e is the amount of heavy metal ions adsorbed per unit mass of adsorbent in mg/g, C_e the equilibrium concentration of heavy metal ions in mg/l, K_f and n are Freundlich constants, 'a' is Langmuir constant which is a measure of adsorption capacity expressed in mg/g, 'b' is also Langmuir constant which is a measure of energy of adsorption expressed in l/mg. The parameters 'a' and 'b' have been calculated from the slope and the intercept of the plots.

The Freundlich adsorption isotherm plot of $\log(q_e)$ versus $\log(C_e)$ is given in (Fig.3.22). The values of K_f and $1/n$ obtained from intercept and slope of the plot are given in (Table 3.9).

The Langmuir adsorption isotherm plot for $1/q_e$ versus $1/C_e$ is shown in (Fig.3.23). The values of **a** and **b** obtained from intercept and slope of the plot are given in Table(3.10)

Table (3.9): Values of Freundlich isotherm for the adsorption of uranium ions by using amidoxime sorbent

No	C_o mg/l	C_e mg/l	Log C_e	q_e mg/g	log q_e
1	100	1.9	0.279	49.05	1.691
2	200	49.9	1.699	74.99	1.875
3	300	130.9	2.117	84.55	1.927
4	350	174.5	2.242	87.75	1.943

Table (3.9 A): Values of Freundlich isotherm constants for the adsorption of heavy metal ions by using amidoxime

Metal ions	Slop(logK_f)	K_f	Intercept(1/n)	n	R^2
U	1.661	45.84	0.128	7.79	0.990

A comparison of the Freundlich adsorption isotherms for the metal ions show that the values of **(n)** lie between 1 and 10 indicating favorable adsorption.

Table(3.10): Values of Langmuir isotherm for adsorption of uranium ions by using amidoxime sorbent.

No	C_o mg/l	C_e (mg/l)	$1/C_e$	q_e (mg/g)	$1/q_e$	C_e/q_e gm/l
1	100	1.9	0.526	49.05	0.020	0.039
2	200	49.9	0.020	74.99	0.013	0.665
3	300	130.9	0.008	84.55	0.012	1.548
4	350	174.5	0.006	87.75	0.011	1.989

Table(3.10A): Values of Langmuir isotherm constants for adsorption of uranium ions by using amidoxime sorbent.

Metal ions	Slop(1/a)	a(mg/g)	Intercept(1/ab)	b(l/mg)	R^2	R_L
U	0.012	86.9	0.017	0.682	0.999	0.015

The essential characteristics of Langmuir isotherm can be described by an equilibrium constant $\boldsymbol{R_L}$, which is defined as,

$$R_L = \frac{1}{1+bC_i} \qquad (12)$$

Where C_i is the initial concentration of heavy metal ions (mg/l) and b is Langmuir constant which indicates the nature of adsorption. The equilibrium constant R_L indicates the isotherm shape and whether the adsorption is favourable or not, as per the criteria given below.

R_L – values	**Adsorption / Type of isotherm**
$R_L > 1$	Unfavorable
$R_L = 1$	Linear
$0 < R_L < 1$	Favorable
$R_L = 0$	Irreversible

The values of Langmuir constants 'a', 'b' and R_L are presented in (Table 3.10A.) Since R_L values lie between 0 and 1 for the amidoxime adsorbant studied, it is seen that the adsorption of uranium is favourable.

The adsorption isotherm studies clearly indicated that the adsorptive behavior of heavy metal ions on amidoxime satisfies not only the Langmuir assumptions but also the Freundlich assumptions, i.e. multilayer formation on the surface of the adsorbent with an exponential distribution of site energy.

Y = 0.128 * X + 1.661
Slop= 1.661 **R^2 = 0.990**
Average X = 1.541 **Average Y = 1.859**

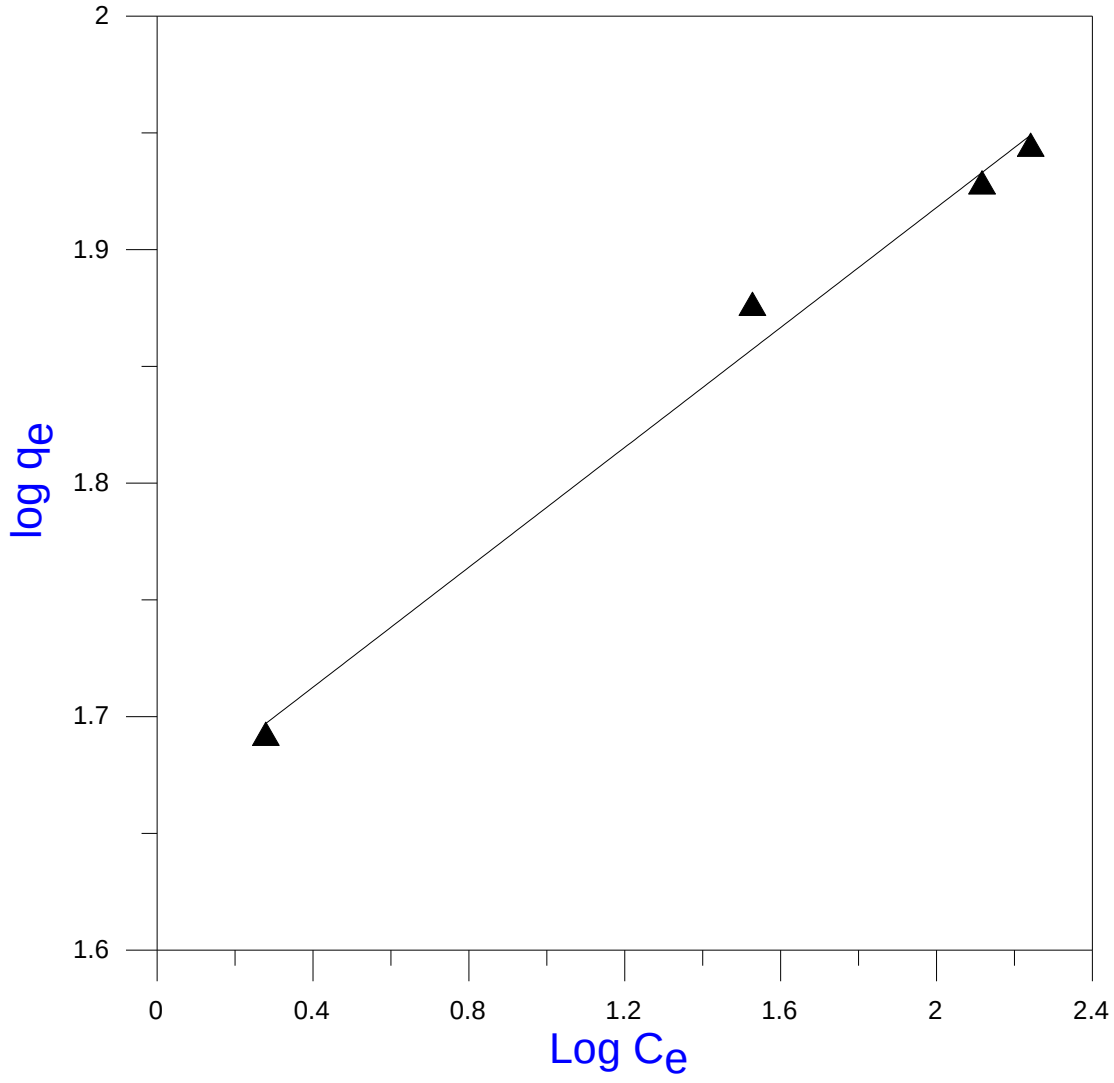

Figure (3.22): Freundlich adsorption isotherm of uranium ions using amidoxime sorbents.

Y = 0.017 * X + 0.012

Slop =0.012 **R^2 = 0.999**

Average X = 0.142 **Average Y = 0.014**

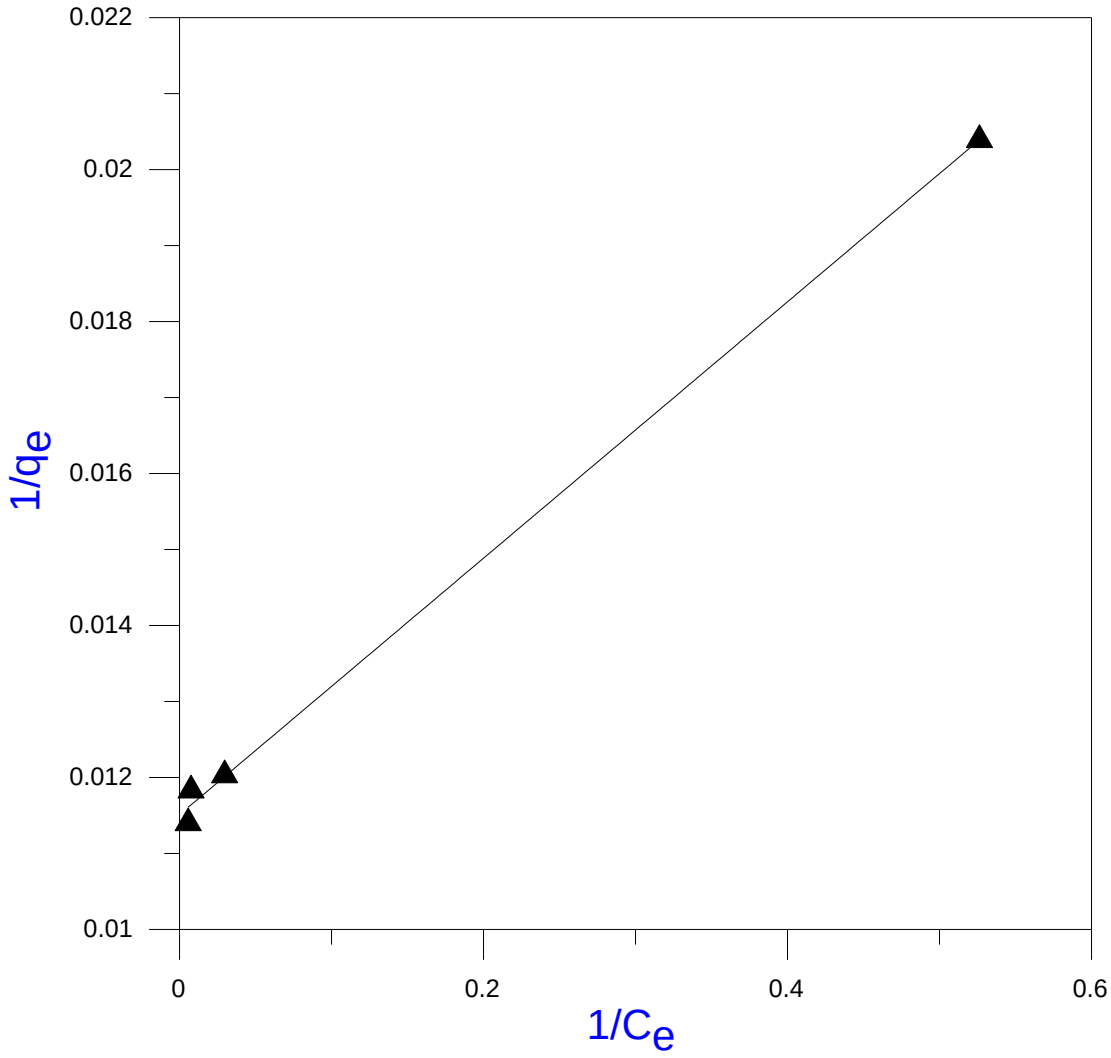

Figure (3.23): Langmuir adsorption isotherm of uranium ions by using amidoxime sorbents.

vii- The adsorption behavior of uranium in presence of some metals ions:

To examine the adsorption behavior of amidoxim chelating starch resin for separation of uranium in absence and in presence of some metals ions: Mg, V, Fe, Ca, Al, Si , Li, Mn, Co, Cd, and Cr , with different concentration of these cations from 25 ppm to 30 ppm. A solution with these specification was prepared from standard reference material (sigma). Adsorption experiments were conducted to determine optimum conditions for uranium behaviour under these conditions. The results are shown in Table(3.11) and Fig.(3.24). The sorption capacities of metal ions by the amidoxime sorbent were found different towards these metal ions. The following order of removal for these impurities are the following ;

Mg>V>Fe>Ca>Al>Si>Li>Mn>Co>Cd>Cr ions.

The presence of this elements reduce the uranium adsorption from 98.8 % to 76.8% due to the presence of these cations as represented in Table(3.11). The experiment conditions of this test are uranium concentration 100 ppm, impurities concentration 30 ppm, pH = 6.5, amidoxime sorbent weight of 0.1g, and shaken time 60 min**.**

Table(3.11): Removal percent of uranium in absence and in presence of impurities elements using amidoxime sorbent.

Elements	Removal percents
U0 alone in clear solution	98.8
U	76.8
Mg	77.9
V	73.0
Fe	71.7
Ca	60.6
Al	52.4
Si	28.6
Li	18.7
Mn	13.9
Co	9.1
Cd	9.0
Cr	1.8

These results indicate that the amidoxime sorbent has a tendency to remove other metal ions than uranium from solution. Among these ions Mg, V, Fe are the most sorbed ions where the %removal is more than 70%. On the other hand, Ca and Al are of moderate sorption tendency where their % removal is between 50 to 60%, while Si, Li, Mn, Co, Cd, and Cr is slightly sorbed.

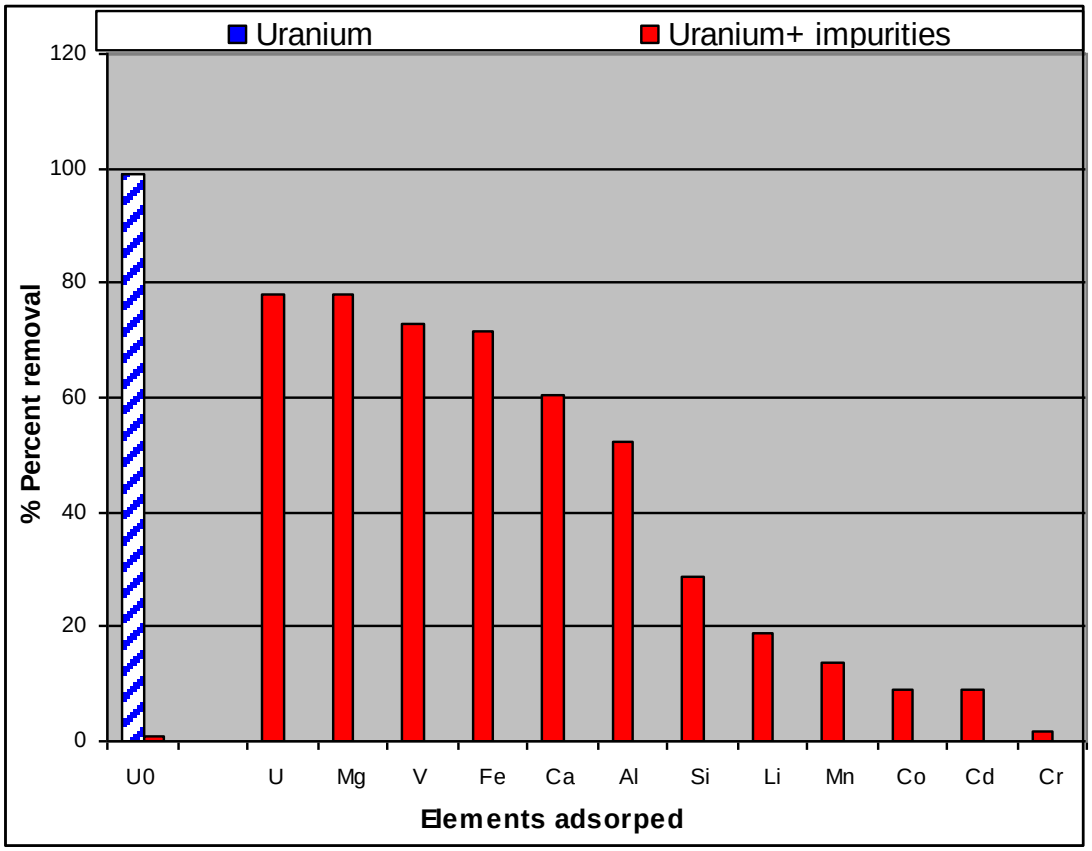

Fig (3.24): The adsorption behavior of uranium in pure solution and uranium in presence of some inspected metals ions using amidoxime sorbent.

vii. Chemical structure of the resulting complex

The specific composition of the complex formed between amidoxime sorbent and U(VI) has not been fully determined. Besides complexes of type 1:2 reported and accepted by many researches [166,167] complexes of type 1:1. 1:3 or 1:4 have also been detected and reported in the literature using data obtained from ^{13}C NMR and ^{1}H NMR. The high capacity for uranium adsorption in a short time is attributed to the complexation and formation of ring structure of amidoxime groups with uranyl ion. Fischer and lieser [168] reported that the amidoxime groups prefer complexation by 6 coplanar donor atoms in equatorial plane of the ion. Three of the amidoxime groups are available to form a chelate with UO_2^{2+} through H_2N--- and HO---- and the coordination number n = 6 gives the optimal distances for this chelation, while, Choi and Nho [169] found that four of the amidoxime groups form chelate with uranyl ion by coordination with four HO- groups and coordination number n = 4 as shown in scheme(3.4)

(a) (b)

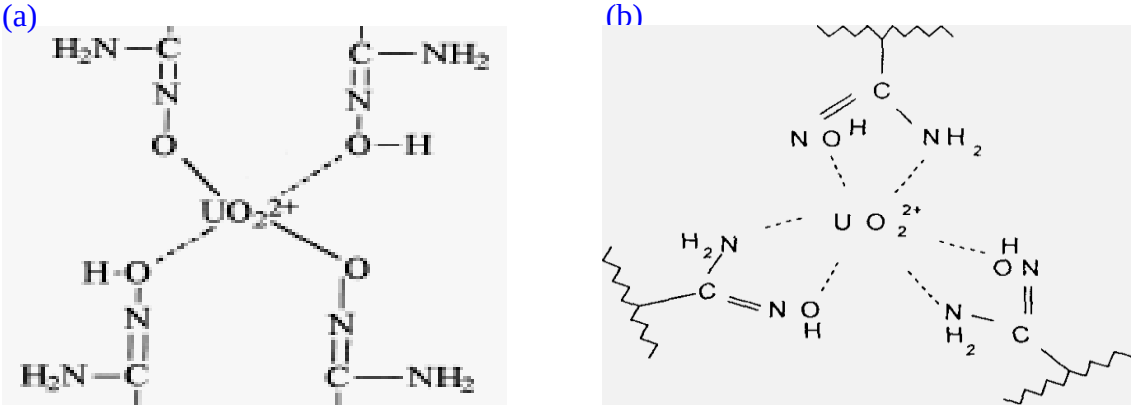

Scheme(3.4): The structure of amidoxime with uranyl ion,(a) coordination n= 4 and (b)coordination n= 6

vi- Morphological Study

The effect of interaction of amidoxime sorbent with uranium ions in the fine structure of the amidoxime sorbent can be studied using scanning electron microscope (SEM). Fig.(3.25a and b) show the SEM photos for the amidoxime sorbent and amidoxime with uranim, respectively. It is clear that the morphology of the amidoxime sorbent containing mainly uranium and other trace elements changed. Sorption of uranium is in the edges of the amidoxime edges.

a- Amidoxim

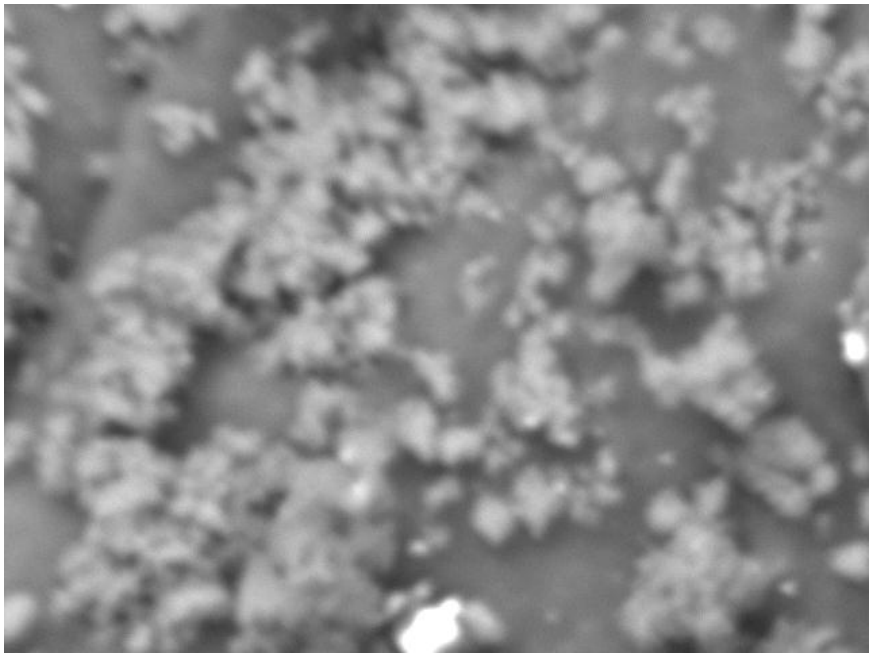

Mag	: x2200
Acc.V	: 15kv
WD	: 20mm
Spot size	: 48

Amidoxime with uranium

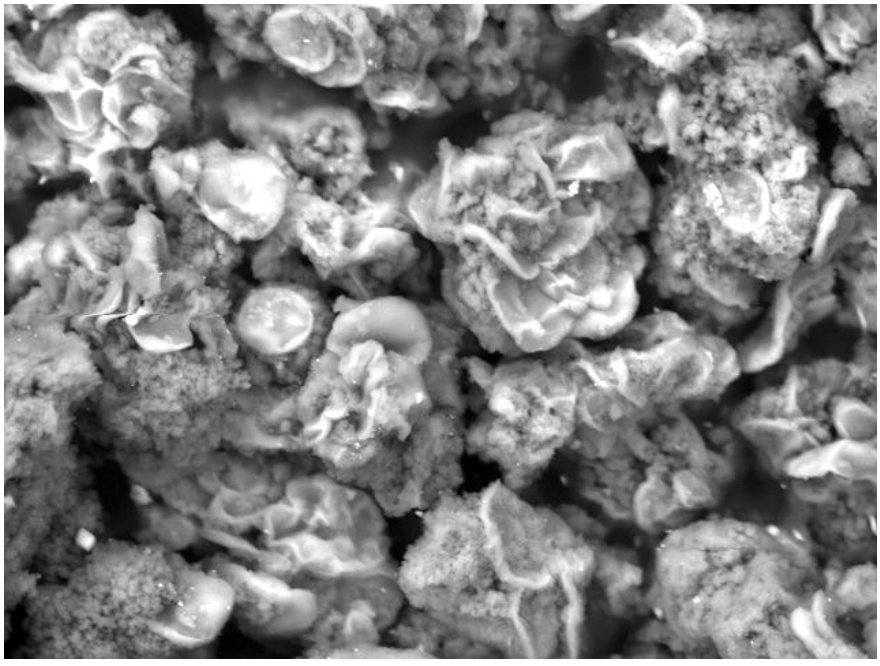

Mag	: x400
Acc.V	: 30kv
WD	: 20mm
Spot size	: 43

Fig (3.25a and b): SEM photos for the (a) amidoxime and (b) amidoxime with uranium ions.

The energy dispersive X-ray spectrometer (EDX) which equipped with the scanning electron microscope (SEM) makes the chemical surface analysis in micro scale possible. Figs.(3.26) and Table (3.12) show the surface analysis of the amidoxime with uranium ion using EDX spectrometer.

Table(3.12): Percentage of elements concentrations in powder samples by EDX

Elements	Concentration %
C	91.7
O	--
Na	0.66
Al	0.29
Si	0.22
Cl	0.81
Ti	---
Fe	0.22
Zn	1.17
U	4.9
Total	100%

There was a detectable amount of U present (EDX analysis), which due to the complexation of uranium with the amidoxime group of the amidoxime sorbent.

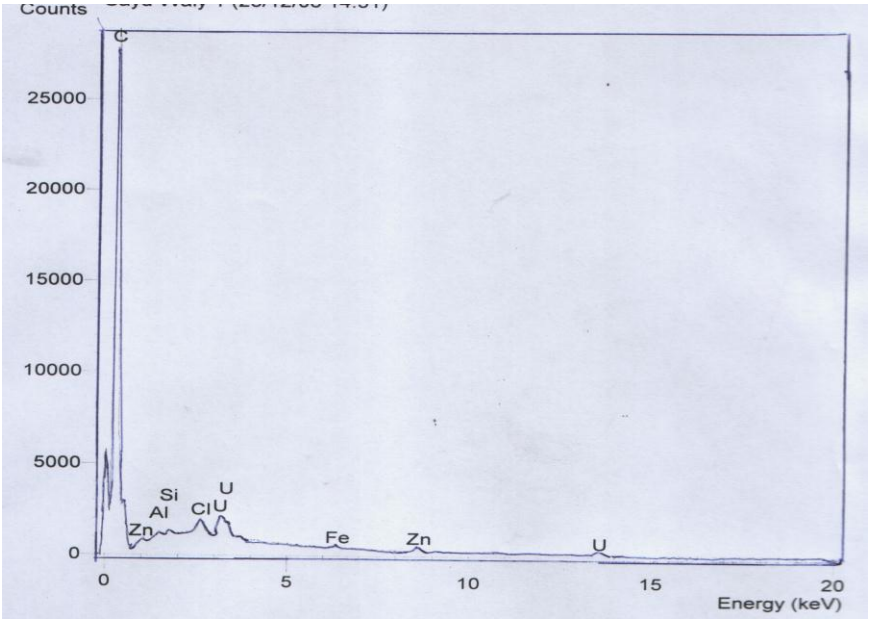

Fig.(3.26): Surface analysis of amidoxime sorbent with uranium using EDX.

3.2.2. Sorption on activated carbon.

Adsorption measurements of uranium by AC were carried out by batch technique. Uranium solution were prepared using U_3O_8 powder. Batch equilibrium studies were carried out by shaking known amounts of activated carbon and uranium solution at room temperature. The solutions were then filtered, and the concentration of uranium was determined spectophotometercally using Arsenazo(III) as given in the experimental.

The experiments were done to investigate the removal of uranium from the waste solution. Unless otherwise stated, all experiments were done under the following conditions : 30 ml of uranium ion solution with concentration 50 mg/l, agitation rate 200 rpm, the solution temperature was 30 ^{0}C and using 0.15 gm of activated carbon having particle size lower than 50µm.

The parameters affecting uranium adsorption on activated carbon were examined.

i- Effect of hydrogen ion concentration, pH.

The influence of initial pH on the adsorption process is shown in Fig (3.26). The pH was adjusted using Na_2CO_3 and HNO_3. The uptake of uranium increases with increasing pH up to 5 and then starts to decrease. Maximum adsorption occurs at pH 5, and hence pH 5 was used in all further studies. The pH dependence of metal ion adsorption is a complex phenomenon and strongly influences the metal ion adsorption. Uranyl ion can combine easily with hydroxyl, carbonate, sulfate and nitrate ions near pH 7, the uranyl ion forms very stable complexes with carbonate. As seen from the figure decreasing adsorption percent may be due to of the formation of $(UO_2(CO_3)_2)^{2-}$and/or $(UO_2(CO_3)_3)^{4-}$ stable complexes [170].

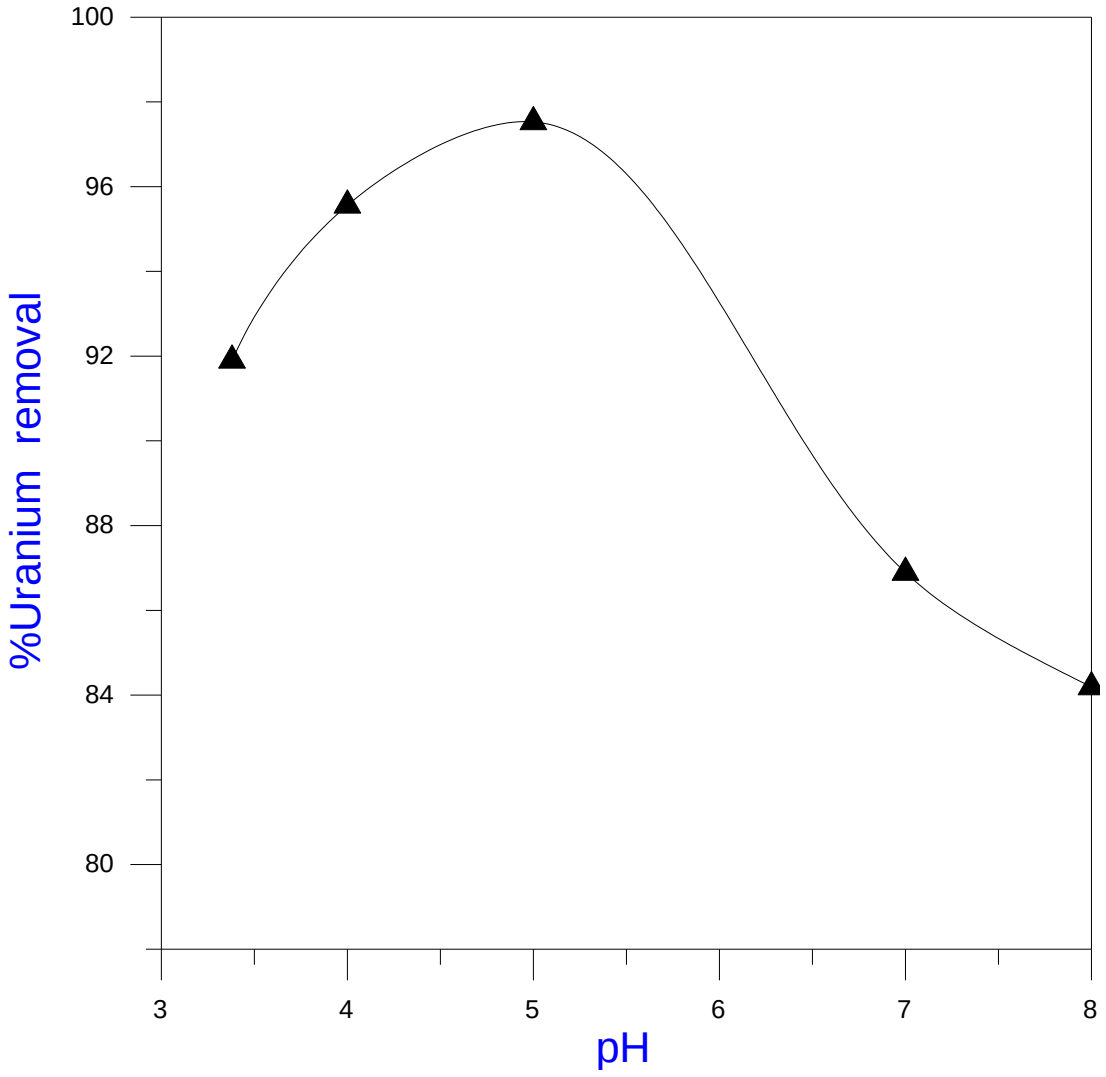

Fig(3.26): Effect of pH on the sorption of uranium by activated carbon.

ii- Effect of shaking time

Sorption of uranium on the prepared activated carbon as a function of shaking time varying from 20-240 min was investigated. Fig. (3.27) gives the relation between the % uranium removal from the aqueous solution against shaking time is given. From this figure it clear that the % uranium removal increase with increasing shaking time to reach a plateau after 60 min. this indicate that equilibrium uptake of uranium is obtained after 60 min. therefore, 60 min was taken for equilibrium removal of uranium.

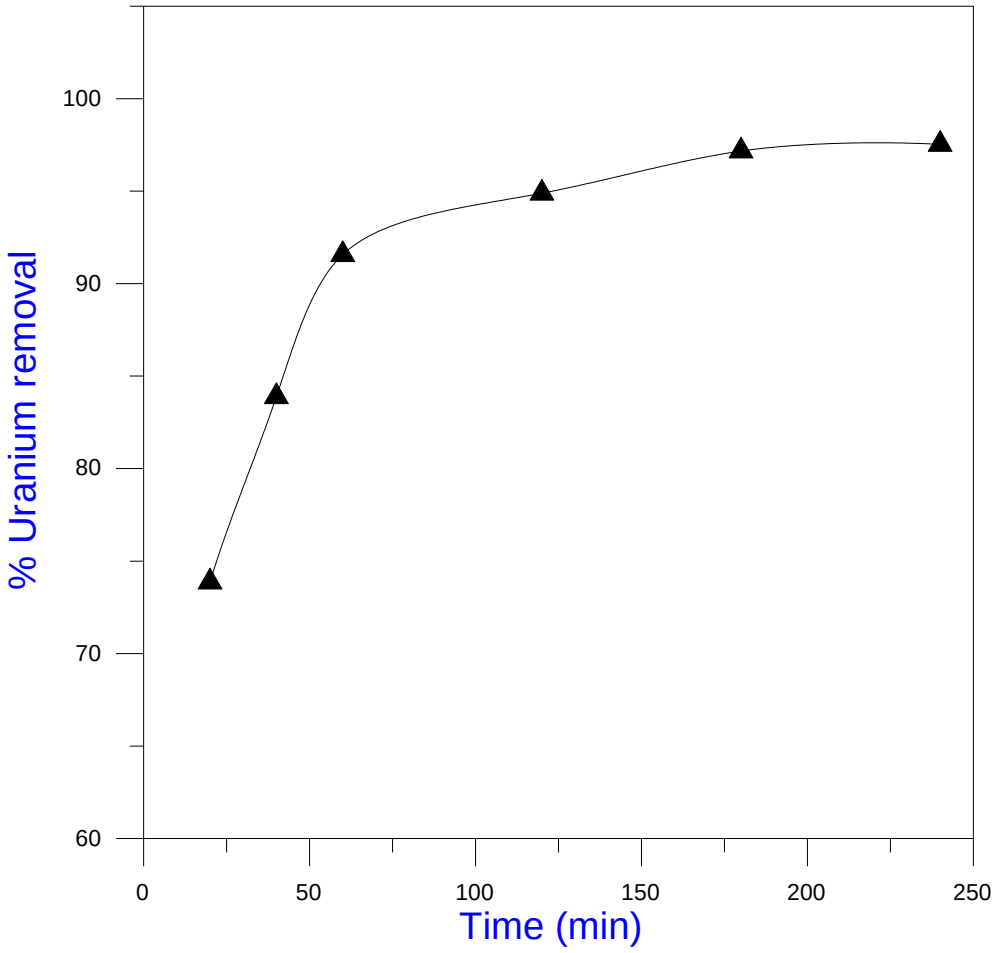

Fig (3.27): Effect of shaking time on the sorption of uranium by A.C (Initial uranium concentration 50 ppm, pH 5 , and wieght 0.15g of adsorbent.)

iii- Effect of sorbent weight

The results of the dependence of uranium adsorption on the amount of sorbent used are shown in Fig (3.28). The volume of solution (30 ml) and, the concentration of uranium (50ppm) were kept constant while the amount of activated carbon varied from 0.05 to 0.2 g. It is seen that an increase in the sorbent weight causes an increase in the uranium adsorption, and reach maximum sorption of 97 % at 0.1 g of AC. Increasing sorbent weight leads to increases the active site of sorbent particles which leads to increases the interaction of uranium ions with this sorbent. Under these condition, the amount of uranium sorped corresponds to sorption of 1.46mg per 0.1g of AC. This corresponds to a sorption capacity of AC of about 14.6 mgU/g AC.

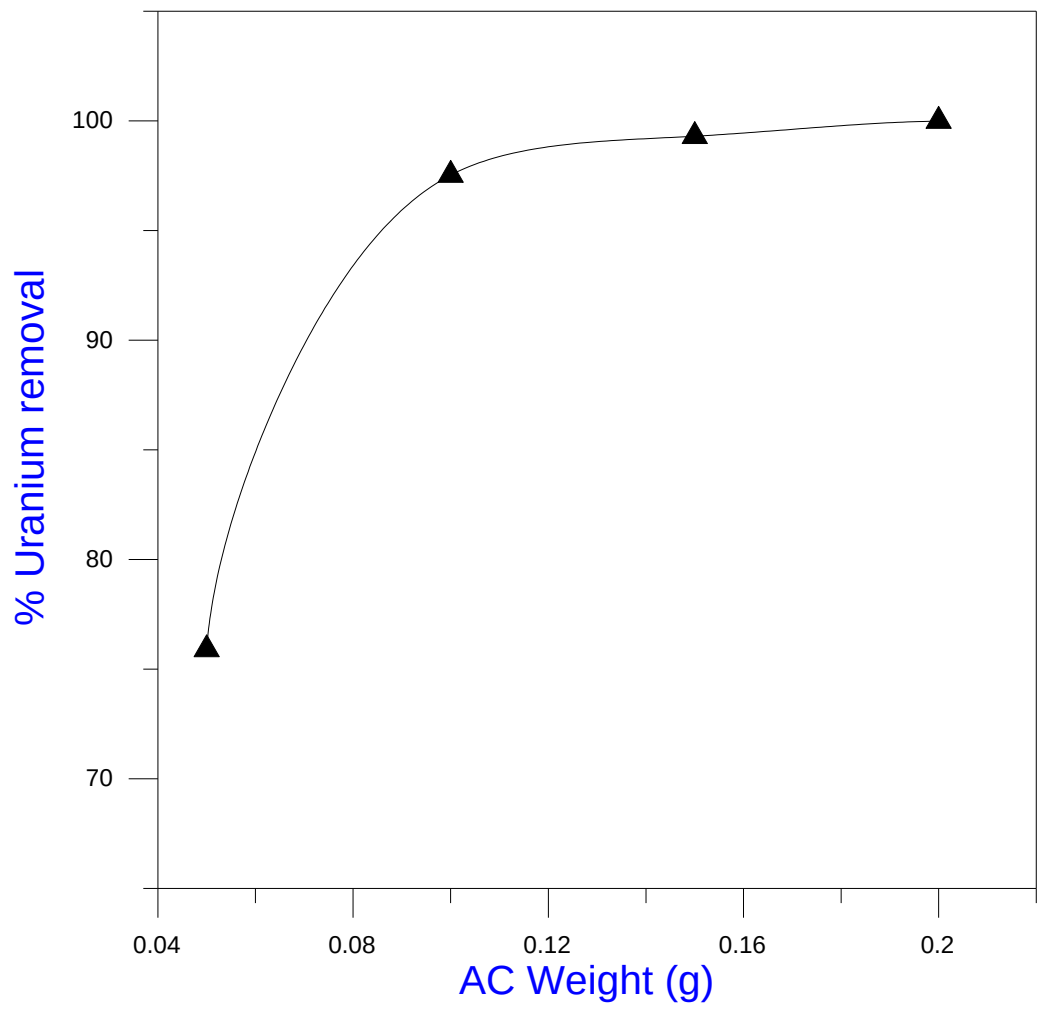

Fig (3.28): Effect of sorbent weight on uranium adsorption by A.C (Initial uranium concentration 50 ppm, pH 5, shaking time:60 min; temperature: 30 ^{0}C).

iv- Effect of temperature

The uptake of uranium by AC at different temperature is given in Fig.(3.29). From this figure it is clear that the % removal of uranium decrease with the increase in the temperature. This indicates that the uptake of uranium by the prepared AC is exothermic. Further, the adsorption of uranium (VI) is favored at low temperatures.

v- Effect of intial uranium concentration

The effect of initial uranium concentration on the % removal of uranium by AC is given in Fig.(3.30a). The uptake of uranium decrease as the uranium concentration increases. Uranium uptake percent is maximum at 50 ppm uranium concentration. Because of the higher mobility of uranyl ions in the diluted solutions, the interaction of the ions with the adsorbent increases. On the other hand, the amount of uranium ions adsorbed per unit of mass of activated carbon (q_e) increase as the uranium concentration increases as shown in Fig (3.30b)

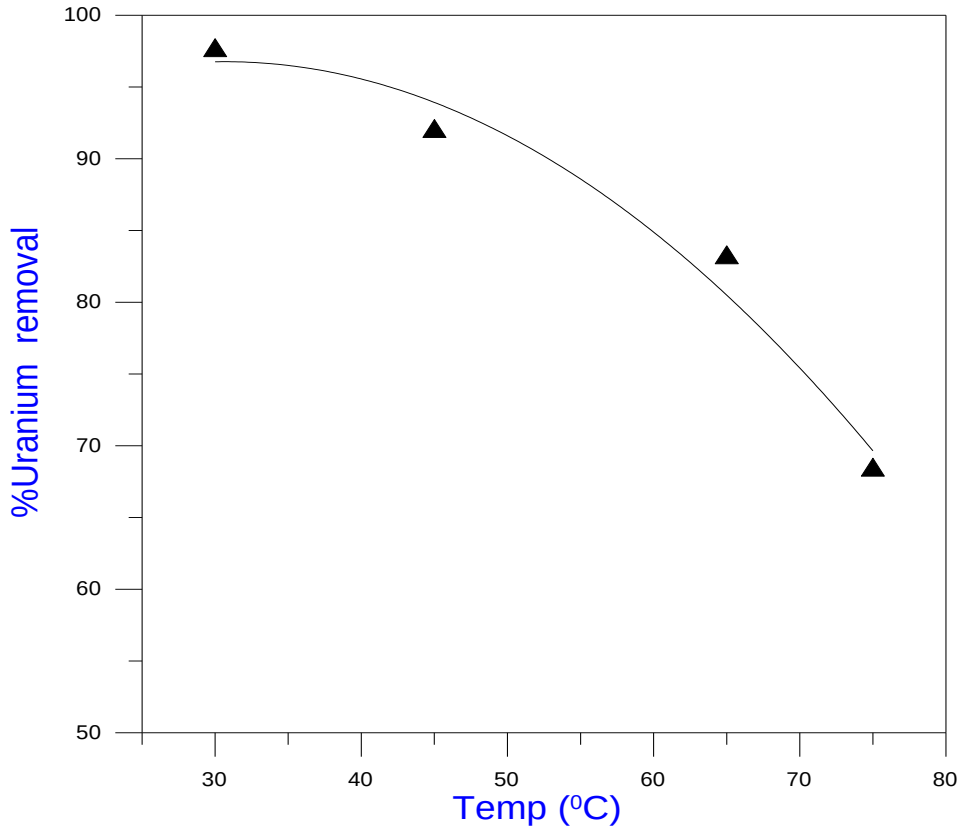

Fig.(3.29): Effect of temperature on the uranium adsorption by AC. (uranium 50ppm, pH 5, AC weight 0.15 g, and shaking time 60 min)

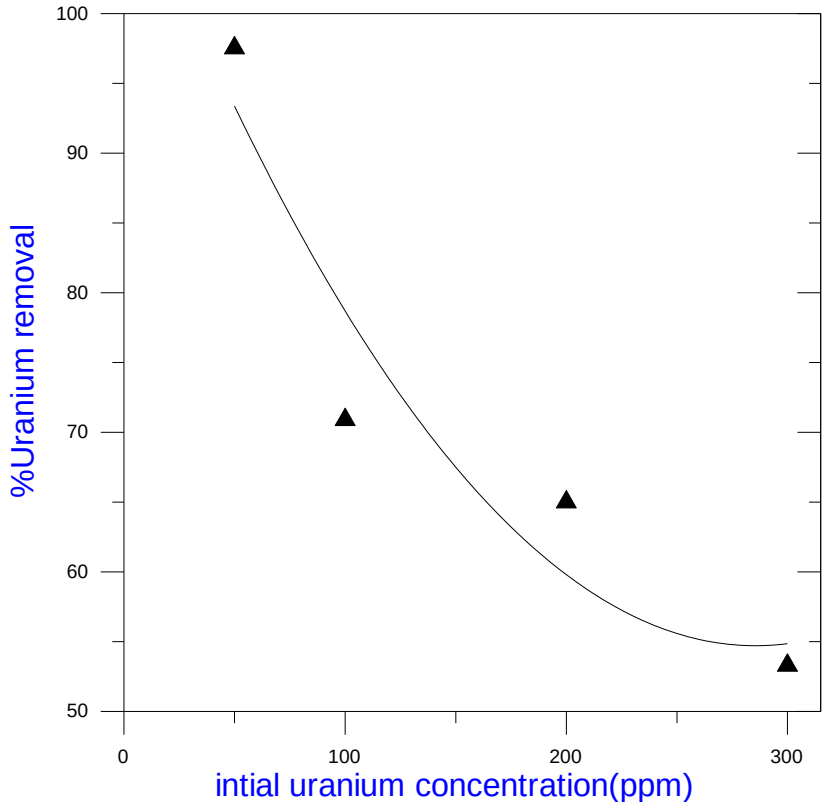

Fig(3.30a): Variation of the percent removal of uranium ions with initial uranium concentration.

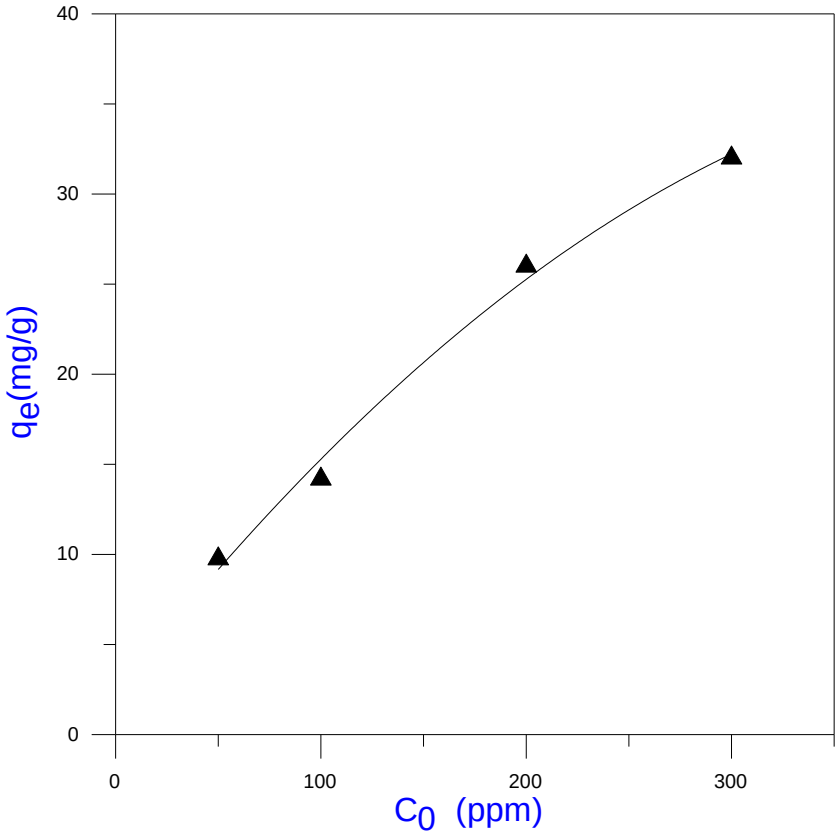

Fig (3.30 b): Variation of amount of uranium ions adsorbed per unit of mass of AC with initial uranium concentration**(**pH 5, shaking time:60 min, and, 0.15g of AC)

vi- Adsorption isotherms of uranium adsorption using activated carbon

In order to understand the adsorption capacity of the adsorbents. the equilibrium data were evaluated according to the Freundlich and Langmiur isotherms, as given in this chapter in case adsorption isotherm of amidoxime sorbent

1-Langmuir isotherm:

The linearized expression of Langmuir equation is

$$\frac{1}{q_e} = \frac{1}{a} + \frac{1}{abC_e} \qquad (11)$$

A linearised plot of C_e / q_e versus C_e: is obtained for activated carbon as shown in Fig. (3.31) and Table (3.13). The fits are well for the activated carbon (correlation coefficient is 0.924). a and b was found as 35.7 mg/g and 0.0445 l/mg, respectively.

Table (3.13): Values of Langmuir isotherm constants for adsorption of uranium ions by using activated carbon

C_o	C_e	$1/C_e$	q_e	$1/ q_e$	C_e/q_e
50	1.2	0.813	9.754	0.103	0.126
100	29.1	0.034	14.18	0.071	2.052
200	70	0.014	26	0.039	2.692
300	140	0.007	32	0.031	4.375

Table (3.13 A): Values of Langmuir isotherm constants for adsorption of uranium ions by using activated carbon

Metal ions	Slop(1/a)	a(mg/g)	Intercept(1/ab)	B(l/mg)	R^2	R_L
U	0.028	35.7	0.630	0.045	0.924	0.310

Y = 0.028 * X + 0.630
Slop= 0.028 **R^2 = 0.924**
Average X = 60.083 **Average Y = 2.311**

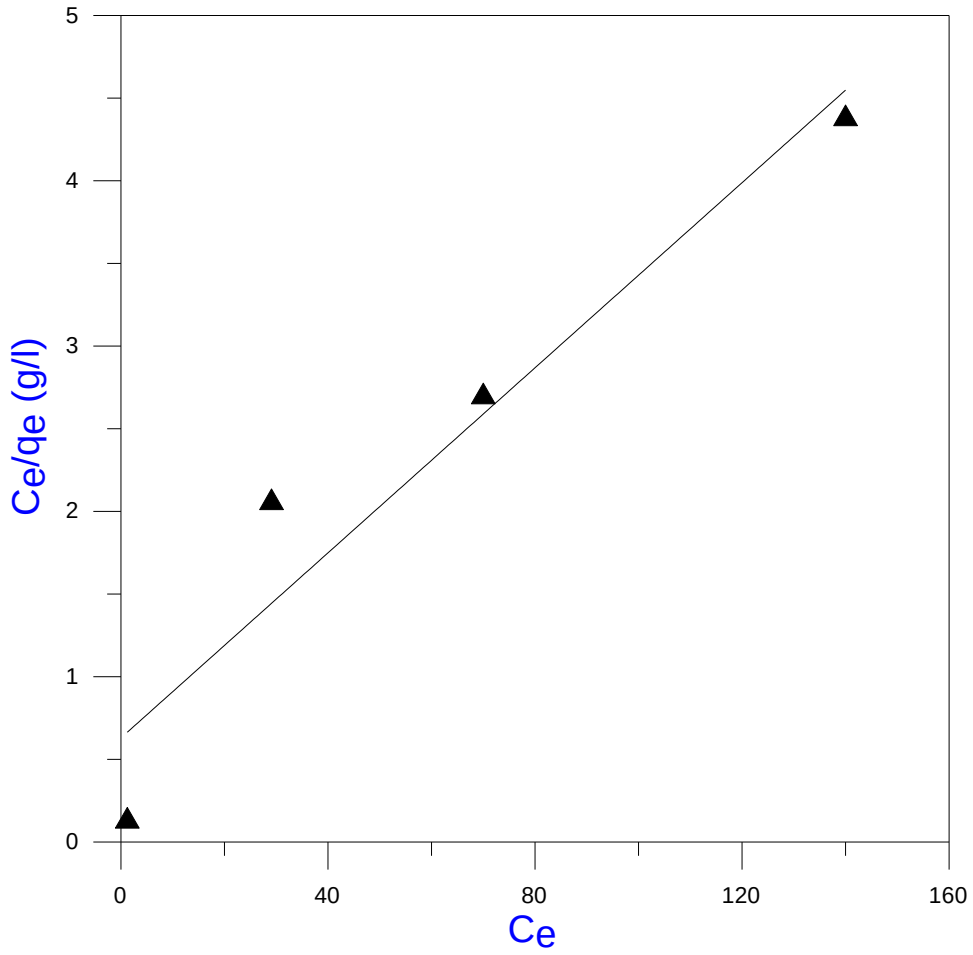

Fig (3.31): Langmuir plot for the adsorption of uranium on activated carbon.

2-Freundlich isotherm

The linearized expression of Freundlich equation is

$$Log(q_e) = Log(K_f) + \frac{1}{n} Log(C_e) \qquad (9)$$

A linearised plot of log q_e versus log C_e is obtained for activated carbon as shown in Fig.(3.32). and table(3.14). The fits are well for the activated carbon. K and n are the Freundlich constants characteristic of a particular adsorption isotherm and can be evaluated from the intercept and slope of the linear plot. The K and n values, respectively, were found to be 8.49 and 4.124 (correlation coefficient= 0.861).

Table (3.14): Values of Freundlich isotherm constants for the adsorption of uranium ions by using activated carbon.

Co	C_e	q	log(qe)	log(Ce)
50	1.2	9.75	0.989	0.090
100	10.9	17.82	1.251	1.046
200	70.0	26.00	1.415	1.845
300	140.0	32.00	1.505	2.146

Table (3.14 A): Values of Freundlich isotherm constants for the adsorption of uranium ions by using activated carbon.

Metal ions	Slop($\log K_f$)	K_f	Intercept(1/n)	n	R^2
U	0.952	8.95	0.246	4.065	0.978

The results suggest that uranium is favorably absorbed by activated carbon prepared from charcoal, Since $\boldsymbol{R_L}$ values lie between 0 and 1 for adsorbants studied, it is seen that the adsorption of uranium is favourable [171].

Y = 0.246 * X + 0.952
Slop = 0.952 **R^2 =0.978**
Average X = 1.386 **Average Y = 1.293**

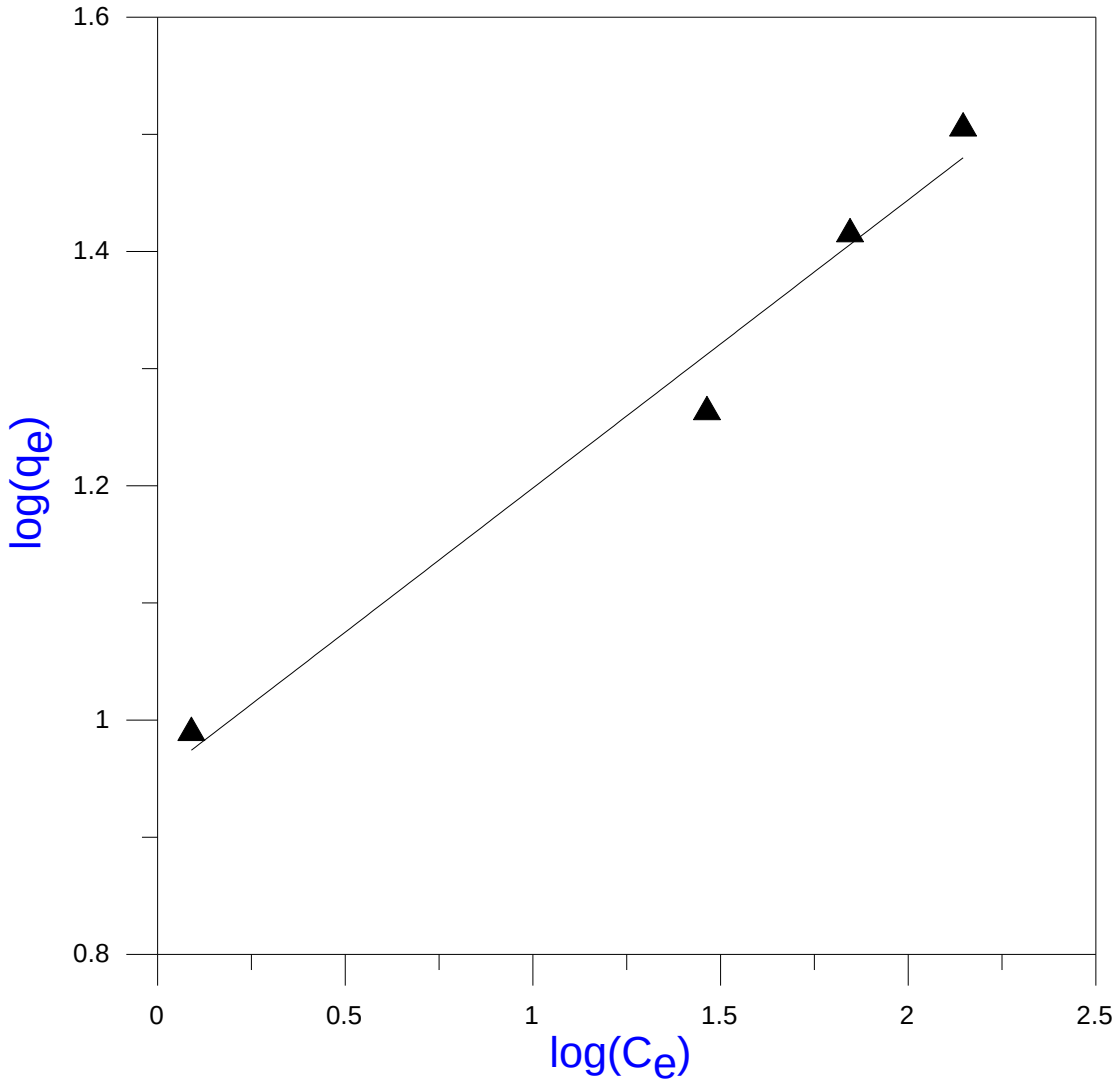

Fig.(3.32): Freundlich plots for the adsorption of uranium on activated carbon.

vi- Morphological Study

The effect of interaction of AC with uranium ions in the fine structure of AC can be studied using scanning electron microscope (SEM). **Figs.(3.33a and b)** show the SEM photos for the AC and AC with uranium, respectively. It is clear that uranium is sorbed in the pores of AC , where Fig (3.33 b) the SEM photo shows that the pores are more or less occupied by uranium sorbed.

(a)AC

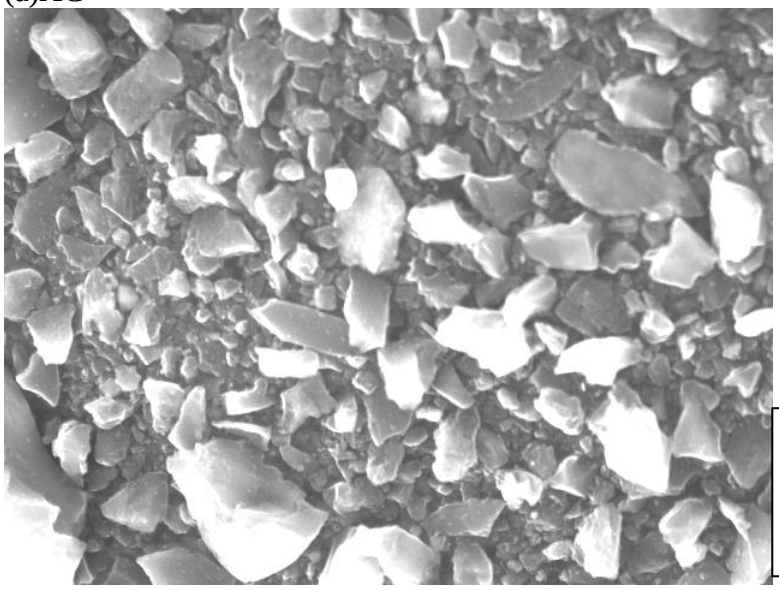

Mga	: x2200
Acc.V	: 30kv
WD	: 8mm
Spot size	: 36

(b) AC with uranium

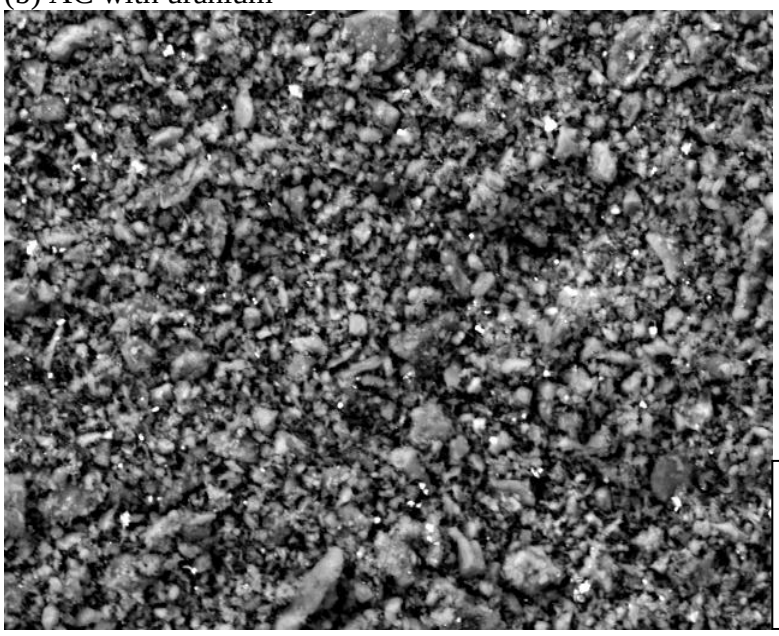

Mga	: x400
Acc.V	: 30kv
WD	: 20mm
Spot size	: 43

Fig (3.33): SEM photos for (a)AC and (b)AC with uranium

3.3. Determination of uranium in different liquid waste streams

One of nuclear research activities in Egypt, the Egyptian Fuel Manufacturing Pilot Plant, FMPP. The main objective of this plant is the production of uranium fuel for the second nuclear research reactor.

3.3.1. The Egyptian Fuel Manufacturing Pilot Plant, FMPP

The Egyptian Fuel Manufacturing Pilot Plant, FMPP, is a new facility, producing an MTR-type fuel elements, with uranium enriched to 19.7% ± 0.2 U^{235}, which is required for the Egyptian Second Research Reactor, ETRR-2.

The production lines in FMPP, which begin from uranium hexaflouride (UF_6, 19.7±0.2 % U^{235} by wt), aluminum powder, and nuclear grade 6061 aluminium alloy in sheets, bars, and rods with the different heat treatments and dimensions as a raw materials, are processed through a series of the manufacturing, inspection, and quality control plan to produce the final specified MTR-type fuel elements as shown in Fig [3.34]. All these processes and the product control in each step are presented. The specifications of the final product are presented. The plant has been designed and built by the cooperation between Argentinean company, INVAP, and Atomic Energy Authority of Egypt.

i- Process Description

- **Evaporation:** The UF_6 is solid at room temperature must be heated over its liquefaction point to increase its vapor pressure.

- **Hydrolysis:** when the gaseous UF_6 is added to the water in a closed agitated vessel a solution of uranyl fluoride and hydrofluoric acid is formed :

$$\mathbf{UF_6\,(v) + 2H_2O\,(l) \rightarrow UO_2F_2\,(sol.) + 4HF(sol.)}$$

- **Precipitation and Filtration of ADU:** Precipitate the solution of UO_2F_2, obtained during the process of hydrolysis by addition of 25% ammonia solution in special condition of temperature and flow rate of ammonia solution, according to the reaction:

$$\mathbf{2UO_2F_2 + 6\,NH_4OH \rightarrow (NH_4)2U_2O_7(solid) + 4NH_4F(sol.) + 3H_2O}$$

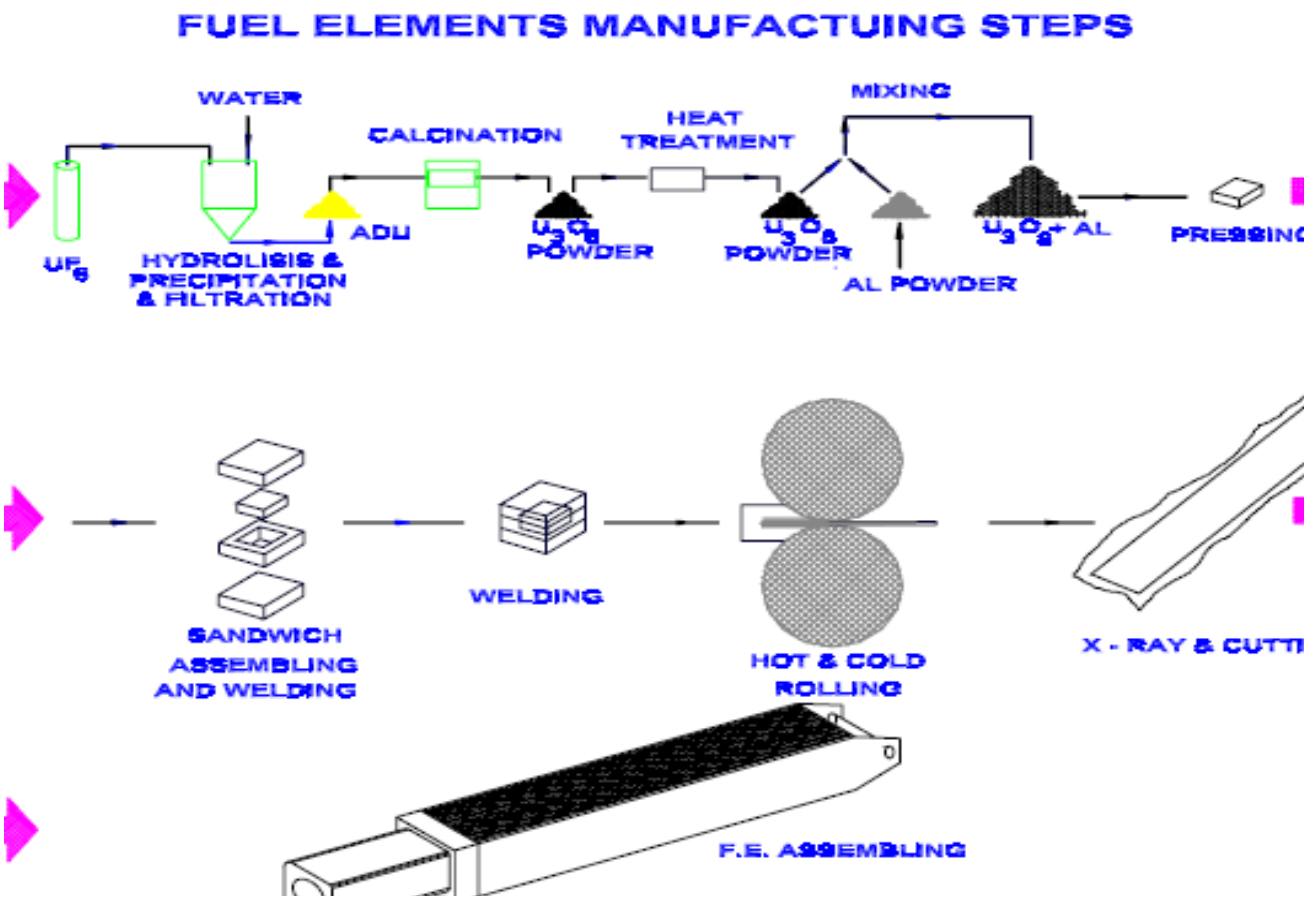

Fig (3.34) The fuel element assembling in FMPP

Filtration of the ADU in suspension, washed with 1% ammonia solution, and dried with alcohol in order to obtain the final ADU.

- **U_3O_8Transformation:** The ADU obtained is calcinated at 800 ^oC to U_3O_8 in an oxidant atmosphere. The product is then milled, the bigger particles broken and smaller agglomerated. After wards it is sized between 44 and 150 microns.

- **Grain growth:** A treatment at 1400^oC is made to obtain the required high density U_3O_8. Subsequently, the material is treated in a mortar, milled and sieved keeping the particles between 44 and 90 microns obtaining the desired product.

ii- Different liquid waste streams in FMPP :

The treatments for liquids originating in the different plant productive activities as shown in schema[3.5], depending on whether or not they contain uranium, are described below.

1- A system for recovering mother liquor generated in the conversion process is available in Area H. This system is designed to concentrate the uranium contained in mother liquors.

The mother liquors is at first U concentration is 50 to 250ppm, and is concentrated to 10 grams/liter by means of an evaporator. Afterwards, the remaining solution should be removed from the evaporator, put into inconal containers and evaporated to dryness over an electrically heated hot plate. Then, the solid waste, is stored in plastic containers in the plant.

2- Other liquid waste in general, with low uranium content, and those originating in Area F (Laboratories) material washing, are collected in two stainless steel tanks with a capacity of a 2000 liters each, fully buried under ground level to allow liquid inlet by gravity. The liquid is pumped from the tank to a special truck, after monitoring, for transportation to AEA's Waste Treatment Plant.

Uranium content was determined by UV-Visible Spectrophotometer as described before in the experimental, afterwards the entire volume of the tanks will be measured into the truck.

The liquid volume generated is lower than 3000 l/year, with an average concentration of less than 10 ppm. This concentration value is below the limit required by the standards.

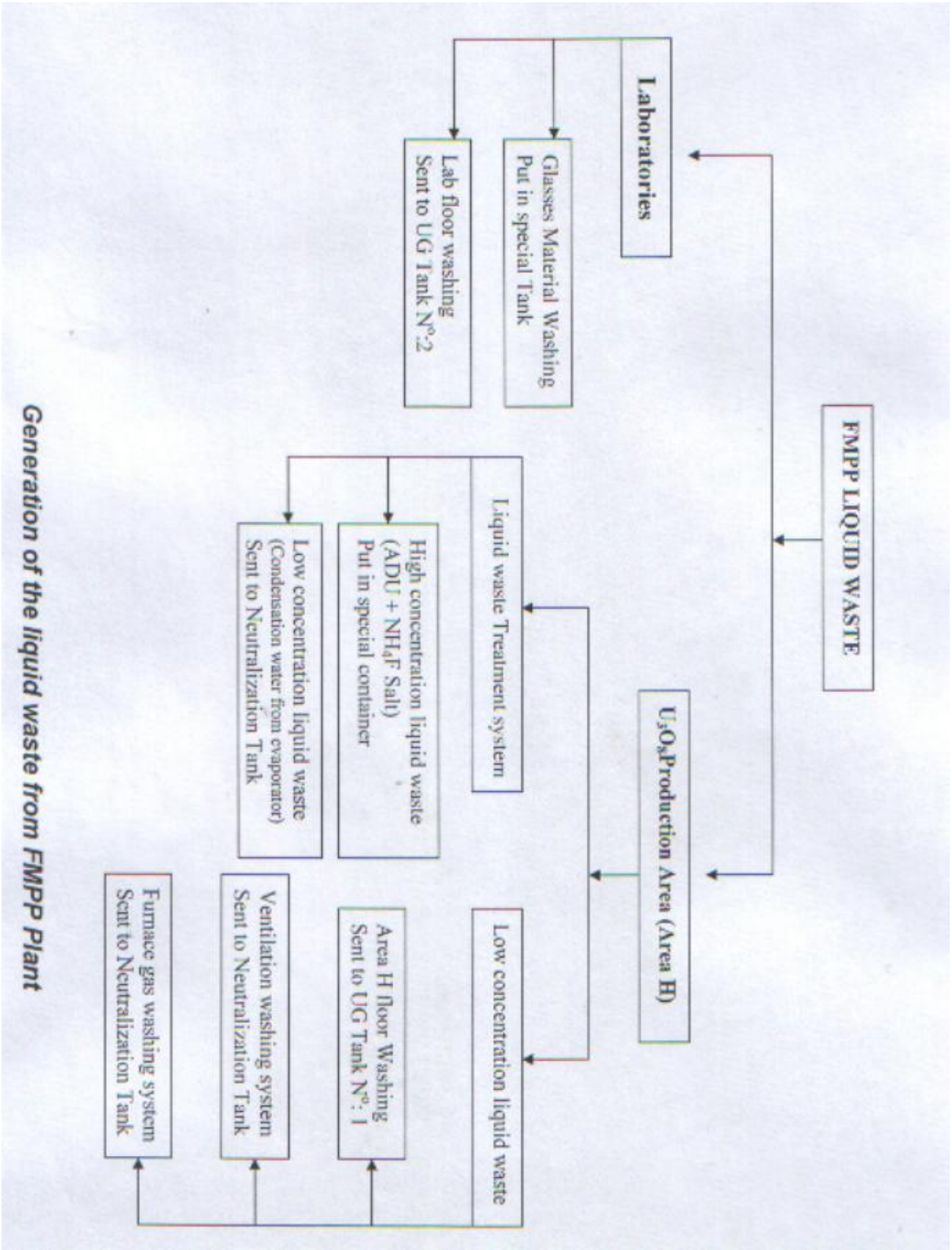

Generation of the liquid waste from FMPP Plant

Scheam (3.6) generation of the liquid waste from FMPP plant.

3.4. Removal of uranium from FMPP liquid wastes using amidoxime sorbent.

It is clear that from the previous results and discussion on the two sorbents prepared namely; amidoxime chelation starch sorbent and activated carbon sorbent, the sorption capacity for amidoxime is found higher than activated carbon. Therefore, the amidoxime chelating sorbent for removal of uranium from FMPP waste was applied for treatment of waste streams of the FMPP plant. The main sources of the FMPP waste, are the chemical laboratory waste, the mother liquor and mother liquor evaporator. These wastes were treated using the amidoxime sorbent under the following experimental condition; 50 ml of waste solution, pH adjusted to 6.5, sorbent weight 0.1g, and shaking time 60 min. Analysis of uranium and impurities before and after adsorption using amidoxime are given in Table (3.15A, and B)

Table (3.15 A): Analysis of waste solutions from different sources of the FMPP plant.

Elements	Conc. FMPP, Lab tank (ppm)	Conc. FMPP, M.L (ppm)	Conc. FMPP, M.L After evaporation (ppm)
U	4.9	15.2	333.7
Co	0.11	0.01	0.03
Cd	0.05	0.98	0.43
Fe	14.94	5.3	14.1
Mn	0.26	0.15	0.31
V	0.02	0.01	0.06
Cr	<0.01	<0.01	<0.01
Si	11.69	1.9	3.1
Mg	8.20	<0.01	<0.01
Ca	95.41	<0.01	0.09
Al	4.67	2.1	3.5
Na	50.77	<0.01	4.7
Li	0.01	<0.01	<0.01
K	3.26	<0.01	<0.01
Ni	0.03	0.3	0.8
B	<0.01	0.01	0.03

Before treatment the waste solution from the laboratory tank source was found to contain 4.9 ppm uranium together with other trace impurities, mainly calcium, sodium, iron, and silicon in concentration a little more than 10 ppm. Concentration of other impurities identified are less the 10 ppm.

After treatment of this solution by amidoxime sorbent, the concentration of uranium in the treated waste solution was found to be 0.01 ppm. This corresponds to a decontamination factor of 99.8%. Other impurities in this solution were reduced, where calcium concentration is 5.41 ppm, sodium concentration is 5.5 ppm, and iron concentration is 1.4 ppm.

Table (3.15 B): Analysis of different sources of FMPP plant after amidoxim sorbent treatment .

Elements	Conc. FMPP, Lab tank (ppm)	Conc. FMPP, M.L (ppm)	Conc. FMPP, After evaporation (ppm)
U	0.01	0.01	93
Co	<0.01	<0.01	<0.01
Cd	<0.01	0.1	0.03
Fe	1.4	1.3	2.1
Mn	0.06	0.03	0.01
V	<0.01	<0.01	<0.01
Cr	<0.01	<0.01	<0.01
Si	1.9	0.1	0.1
Mg	1.2	<0.01	<0.01
Ca	5.41	<0.01	0.1
Al	0.7	0.1	1.1
Na	5.5	<0.01	0.9
Li	<0.01	<0.01	<0.01
K	0.06	<0.01	<0.01
Ni	<0.01	0.1	0.1
B	<0.01	<0.01	<0.01

Analysis of liquid waste produced from the mother liquor, (M.L) showed that uranium concentration is 15.2 ppm. The main impurities in this waste solution is iron with a concentration of 5.3 ppm, aluminum 2.1 ppm, silicon 1.9 ppm, and cadium 0.98 ppm. After treatment, the concentration of uranium in the treated waste solution was found to be 0.01 ppm. This corresponds to decontamination factor of 99.9%. Other impurities in this solution were reduced, where iron concentration is 1.3 ppm, and aluminum concentration is 0.1 ppm.

Analysis of liquid waste produced from the mother liquor after evaporation showed that uranium concentration is 333.7 ppm. The main impurities in this waste solution is iron with a concentration 14.1 ppm, sodium 4.7 ppm, and aluminum concentration is 3.5 ppm. After treatment, the concentration of uranium in the treated waste solution was found to be 93 ppm. This corresponds to decontamination factor of 72.1%. Other impurities in this solution were reduced, where iron concentration is 2.1 ppm, sodium 0.9 ppm, and aluminum concentration is 1.1 ppm.

These results indicate that the treatment process is efficient to remove uranium from the waste solution of the FMPP plant and a developments of a semi-pilot plant for treatment of these waste is promising

Summery and Conclusion

The present work is mainly concerned with the synthesis of suitable sorbent for removal of uranium from liquid waste streams of The Egyptian Fuel Manufacturing Pilot Plant, FMPP which is a new facility, for the production of the Material Testing Reactor, MTR-type fuel elements, enriched to 19.7% ± 0.2 U^{235}. This is required for the Egyptian Second Research Reactor (ETRR-2) in Atomic Energy Authority.

Therefore, the main aim of this work is to prepare suitable sorbent based on amidoxime or activated carbon for removal of uranium from the waste streams of the FMPP plant. Therefore, the work carried out in this thesis is presented in three main chapters.

Chapter 1;

The introduction includes a background on the toxicity of uranium and its presence in radioactive waste solutions in waste streams of uranium fuel production plants. An outline on the different techniques used for separation with special reference to adsorption methods and equilibrium adsorption methods are given. A special part on the grafting polymerization for preparation of polymeric sorbents is also outlined. Basic methods for analysis in terms of accuracy, precision, sensitivity, scale of operation and equipment are given. Literature surveys for recent works on the removal of uranium from waste effluent using amidoxime or activated carbon are reported.

Chapter 2;

The experimental contains the different chemical used, the methods for preparation of the sorbents, and different techniques used for characterization and measurement of different parameters.

The first sorbent is amidoxime prepared by grafting reaction of starch, the backbone of the polymer, with AN which was carried out by two methods, namely; free radical initiation and radiation induced polymerization, followed by treatment of nitrile copolymer with hydroxylamine.

The second sorbent is activated carbon prepared by chemical activation for charcoal using $ZnCl_2$ solution then heated to carbonization temperature.

Different apparatus used for chemical and physical analysis, namely UV-Visible spectrophotometer and inductively coupled plasma atomic emission spectrometer for elemental analysis, scanning electron microscope and micrometric sedigraph 5100 for particle size analysis and micromeritics gemini 2360 for surface area analysis are described. The experimental procedures for analysis and calibration using standard reference materials as well as sorption investigation are also included.

Chapter 3;

Results and discussion consist of three main parts. The first is concerned with the preparation and characterization of the prepared sorbents. In this respect, the amidoxime sorbent was prepared by two methods. In the first, chemical intiation was used for grafting acrylonitrile with starch by initiation with ceric ammonium nitrate. In the second, radiation grafting was used for polymerization of starch with acrylonitrile monomer. Within this merits, starch and acrylonitile monomer were irradiated by a dose of 15 kGy of the γ- ray from Co-60 source at a dose rate of 2.5 k Gy/h. It is found that the grafting efficiency using radiation is much higher than that by chemical grafting. The amidoxime chelating starch sorbent was characterized in terms of the starting materials (Starch and PAN) and the final product. These materials were investigated using elemental analysis, particle size distribution, surface area, IR spectrum, thermo-gravimetric analysis and morphology. The particle size of the prepared amidoxime sorbent was found to equal 90.2 μm and its surface area equals 8.1 m^2/g.

The second prepared sorbent is the activated carbon. Activated carbon was prepared from charcoal by chemical activation. The preparation process consisted of zinc chloride impregnation followed by carbonization. The carbonization temperature ranges from 500 to 700 ^{0}C for 1 h. Activated carbon was characterized using particle size distribution, surface area, and morphology study. The produced AC showed a particle size of 35 μm and surface area of 581.2 m^2/g.

The second part of this thesis is concerned with sorption of uranium by the prepared sorbents. The sorption of uranium by the prepared sorbents, amidoxime sorbent and activated carbon were investigated in terms of the changes in pH, shaking time, resin weight, temperature and initial uranium concentration.

It is found that the % removal of uranium by the sorbents is dependent on the hydrogen ion concentration of the medium. In case of amidoxime sorbent, maximum uptake of uranium was found at pH 4-6.5 where by AC, maximum uptake was found at pH 5. Equilibrium uptake was attained after 60 min for the two sorbents used. The results showed that the capacity of amidoxime for uranium (86.9 mg/g) is higher than that of AC (35.7mg/g). The effect of temperature indicated that the sorption increase with temperature using amidoxime where by the sorption decrease with temperature in the case of AC.

It is to be mentioned that during the different preparation, characterization and sorption experiments, the different analytical methods were assessed. It is found that for trace element analysis there are high agreement for uranium analysis using colorimetric method based on UV-Visible method and ICP-AES. Concerning particle size distribution measurements, it is found that use of sedigraph 5100 unit, based on falling of dispersed particles followed by x-ray counting, is more accurate than SEM measurements.

The adsorption isotherms of the experimental results were analyzed by Freundlich and Langmuir models**.** These models explained the sorption results satisfactorily. Further, the Freundlich constants obtained are K_f =45.84 and n= 7.79 where by in the case of Langmuir constant are a=86.9 and b=0.682. These indicated that the sorption of uranium is favorable. Further, a chemical mechanism was proposed for uranium.

For activated carbon sorption results, the aforementioned models were also applied. Both models explained the sorption behavior of uranium by AC. Further, the Freundlich constants obtained are K_f =8.95 and n= 4.065 and that for Langmuir are a=35.7 and b=0.045. These constants for AC are less than that for amidoxime and indicated that sorption of uranium by amidoxime is more favorable than the prepared AC.

It is clear that from the previous results and discussion on the two sorbents prepared namely; amidoxime chelating starch sorbent and activated carbon sorbent, the sorption capacity for amidoxime is found higher than activated carbon. Therefore, the amidoxime chelating sorbent for removal of uranium from FMPP waste was recommended for treatment of waste streams of the FMPP plant.

The third part of the results and discussion is concerned with the use of amidoxime sorbent for removal of uranium from FMPP waste streams of the FMPP plant. In this concern, the flow diagram for production of the fuel elements is given and the different waste streams within the facility of the FMPP plant are outlined. The main sources of the FMPP waste are the chemical laboratory waste, the mother liquor and mother liquor after evaporation. After treatment of waste streams of FMPP using the amidoxime sorbent, the decontamination factor is found 99.8% for chemical laboratory waste, 99.9% for mother liquor, and 72.1% for mother liquor after evaporation.

This indicate that the treatment process based an amidoxime sorbent is efficient to remove uranium from the waste solution of the FMPP plant to achieve the main aim of work.